Juhan Ross Legacy Symposium, Aug 24-25 2017

https://jrls2017.to.ee/

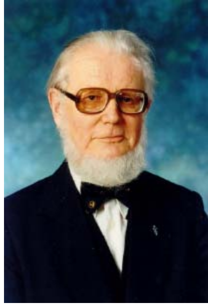

A unified radiosity model for optical and microwave regions

Huaguo Huang

College of Forestry, Beijing Forestry University

Huaguo.huang@gmail.com; huaguo_huang@bjfu.edu.cn

北京林业大学

Outline

1. Where RAPID comes from?
2. Objective and motivation
3. Unification method selection
    a. Reviewing modeling strategies
    b. How to bridge optical and microwave
4. RAPID2 (Radiosity Applicable to Porous IndiviDual Objects)
    a. Basic theory of radiosity
    b. 3D Scene description
    c. Radiative transfer processes in all bands
5. Validation
6. Summary

1. Where RAPID comes from?

My Ph.D. supervisors:

- **Xiaowen Li** (Geometric Optics Model)
- Qinhuo Liu (link to Qin in NASA/GSFC)
- **Wenhan Qin** (RGM, 2000) ← Goel (DIANA,1991)

I am in the boat of radiosity theory

- TRGM (thermal RGM, 2007)
- LRGM (large RGM, 2009)—RAMI-IV (RGM2)
- RAPID (rapid RGM, 2013)
- Now RAPID2

REMOTE SENS. ENVIRON. 36:73–104 (1991)

A Computer Graphics Based Model for Scattering from Objects of Arbitrary Shapes in the Optical Region

DIANA model

*Narendra S. Goel, Ivan Rozehnal, and Richard L. Thompson**

Department of Systems Science, State University of New York, Binghamton

1. Created a modified L system to objects of arbitrary shapes

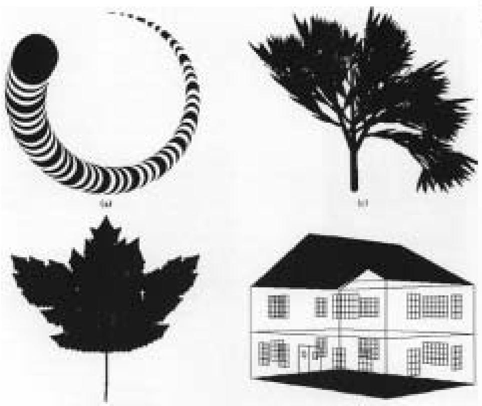

Figure 4. A representative selection of objects generated using L-systems.

Figure 5. A corn canopy generated by a stochastic L-system (from Goel, Knox and Norman, 1991).

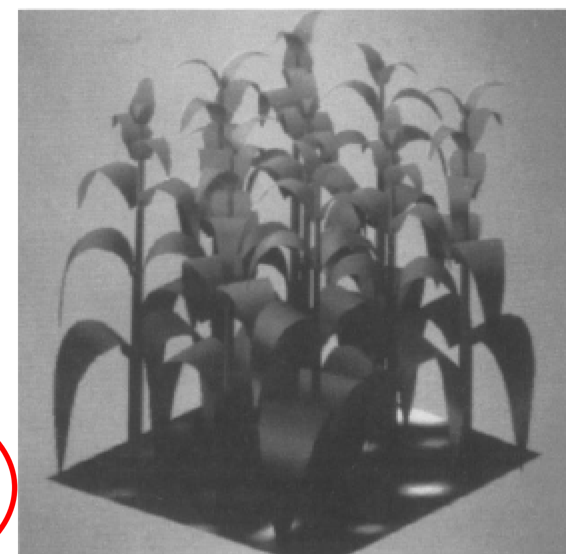

2. Developed a complete radiosity framework for plants with high transmittance under outdoor light environment

$$B_i = E_i + \rho_i \sum_{j=1}^{N} B_j F_{ij} + \tau_i \sum_{k=1}^{N} B_k T_{ik},$$

REMOTE SENS. ENVIRON. 74:145–162 (2000)

3-D Scene Modeling of Semidesert Vegetation Cover and its Radiation Regime

RGM

Wenhan Qin and Siegfried A. W. Gerstl†*

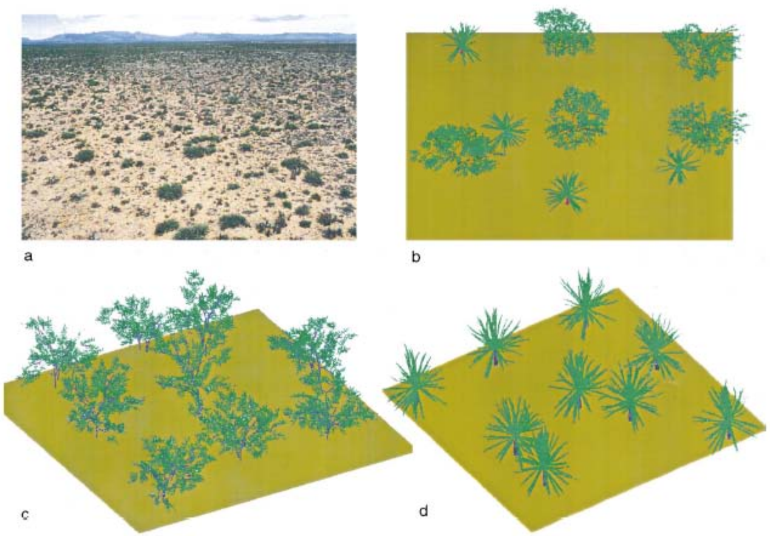

Figure 1. A photograph taken from the top of the tower at the study site (a) versus a sample of MELS-rendered Jornada scene (b) and its components [(c) mesquite, (d) yucca].

1. Extended DIANA to calculate
   FPAR
   hyper-spectral BRF
   FOV effect

2. Full validations on semi-desert vegetation

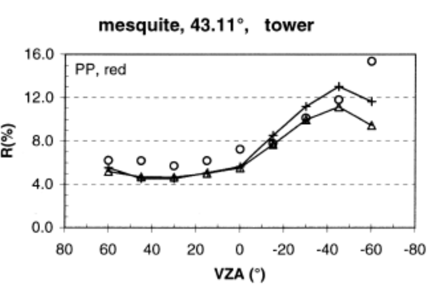

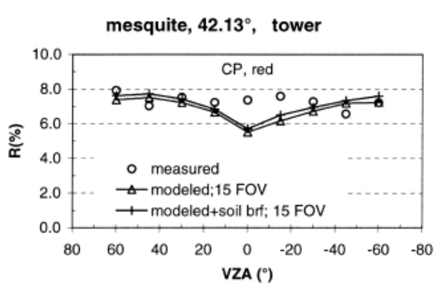

New advances of RAPID2

- 3D scenes: easy to use GUI, more simplification
- Atmosphere: RAPID-VLIDORT (Huang, GRSL, 2017)
- 3D temperature: RAPID-ENVI-met (IGARSS, 2015)
- New sensors:
  - Lidar waveform (CJRS, 2013)
  - point cloud
  - CCD image, push-broom image
  - Ground goniometer using perspective projection

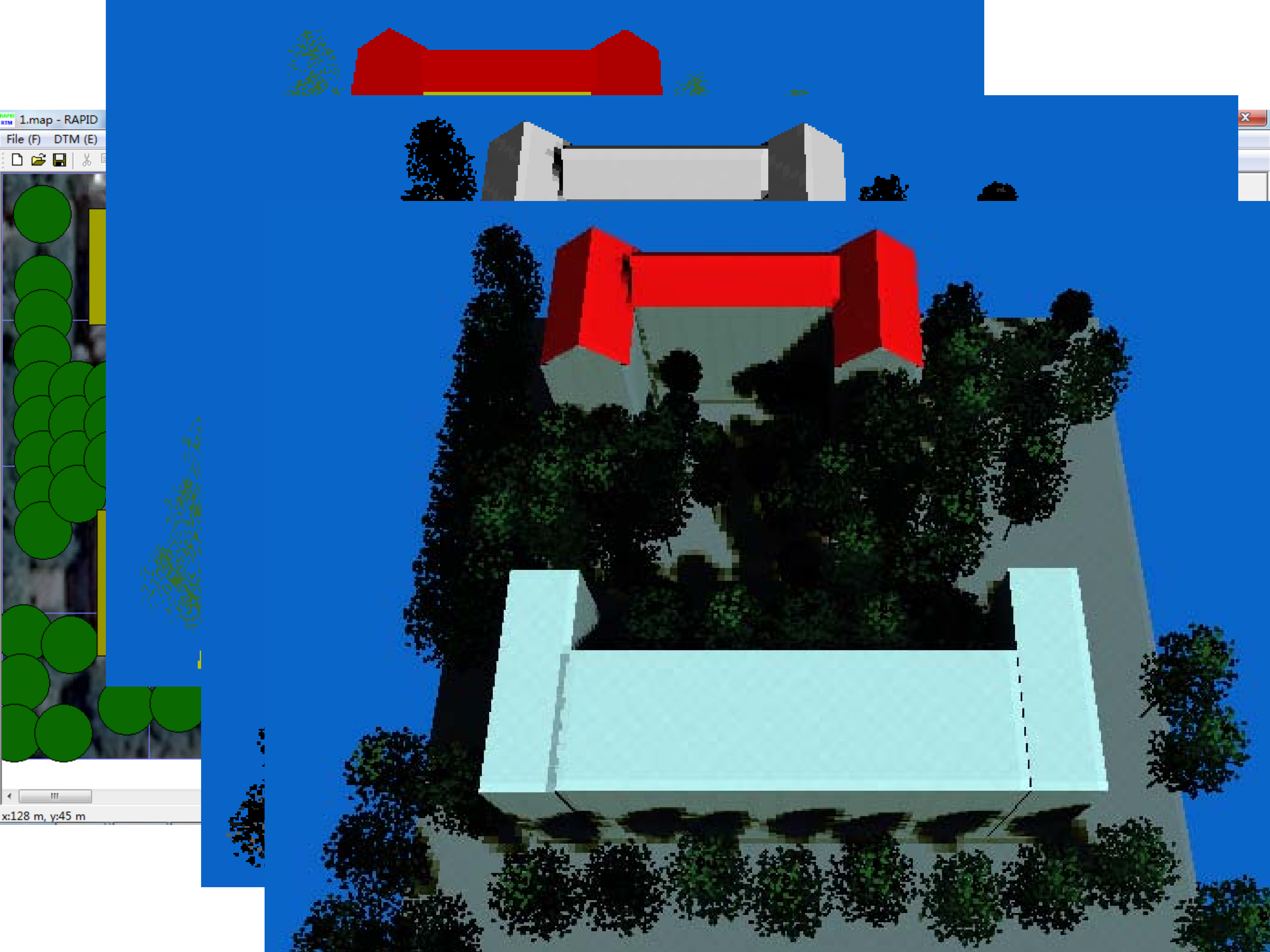
1.map - RAPID
File (F)
DTM (E)
x:128 m, y:45 m

Simulating fish-eye images in RGB, NIR, and TIR

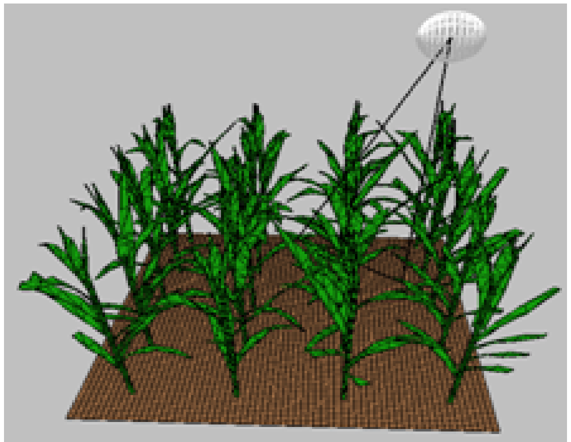

(a)

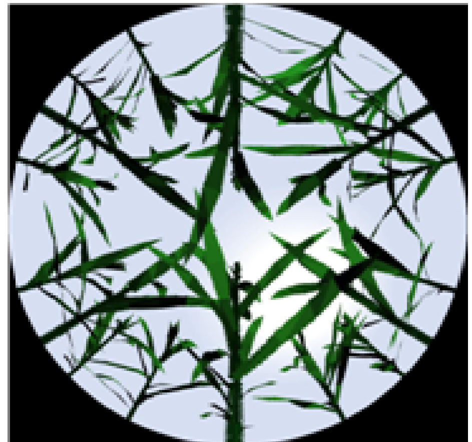

(b) RGB

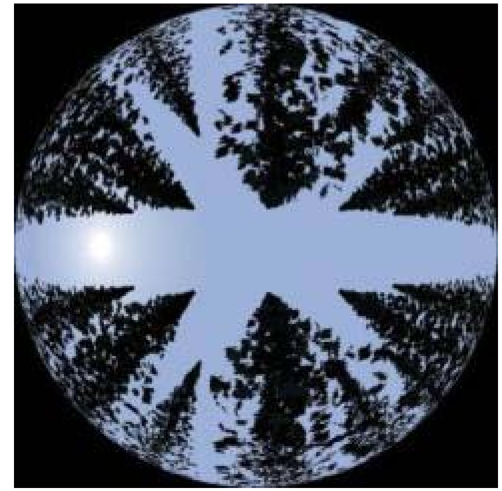

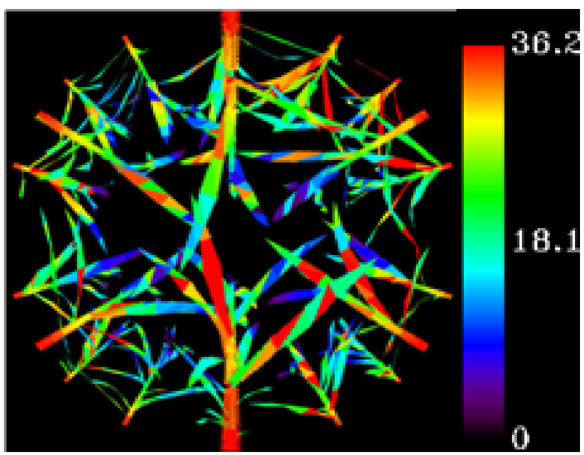

(c) TIR

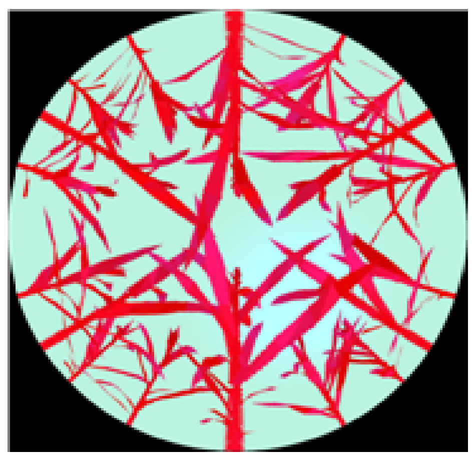

(d) NIR

黄华国，2011，系统仿真学报

Lidar point cloud simulation

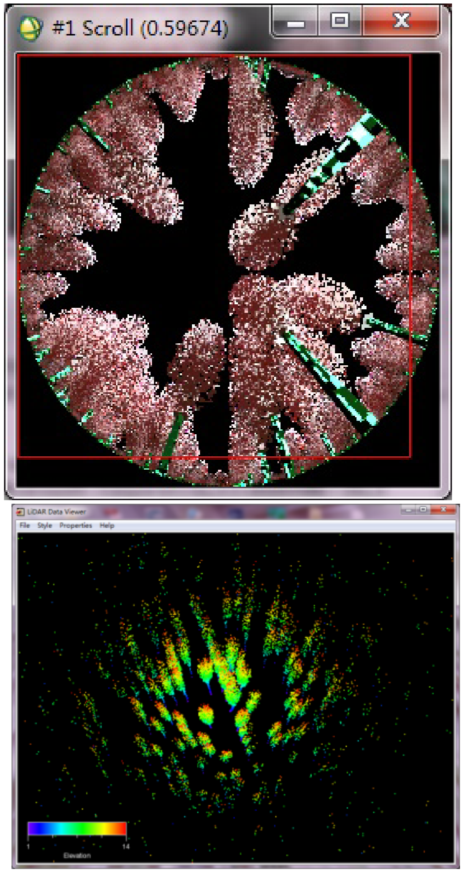

TLS below canopy

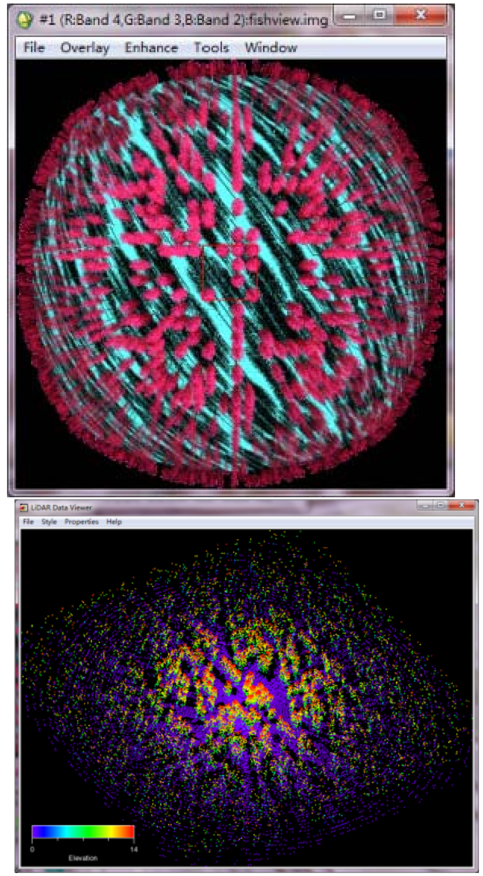

TLS above Canopy 10m

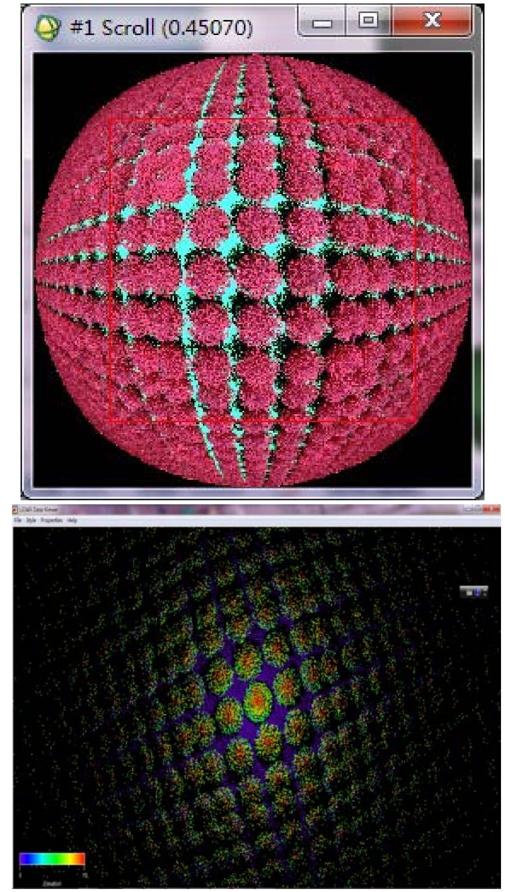

TLS above Canopy 50m

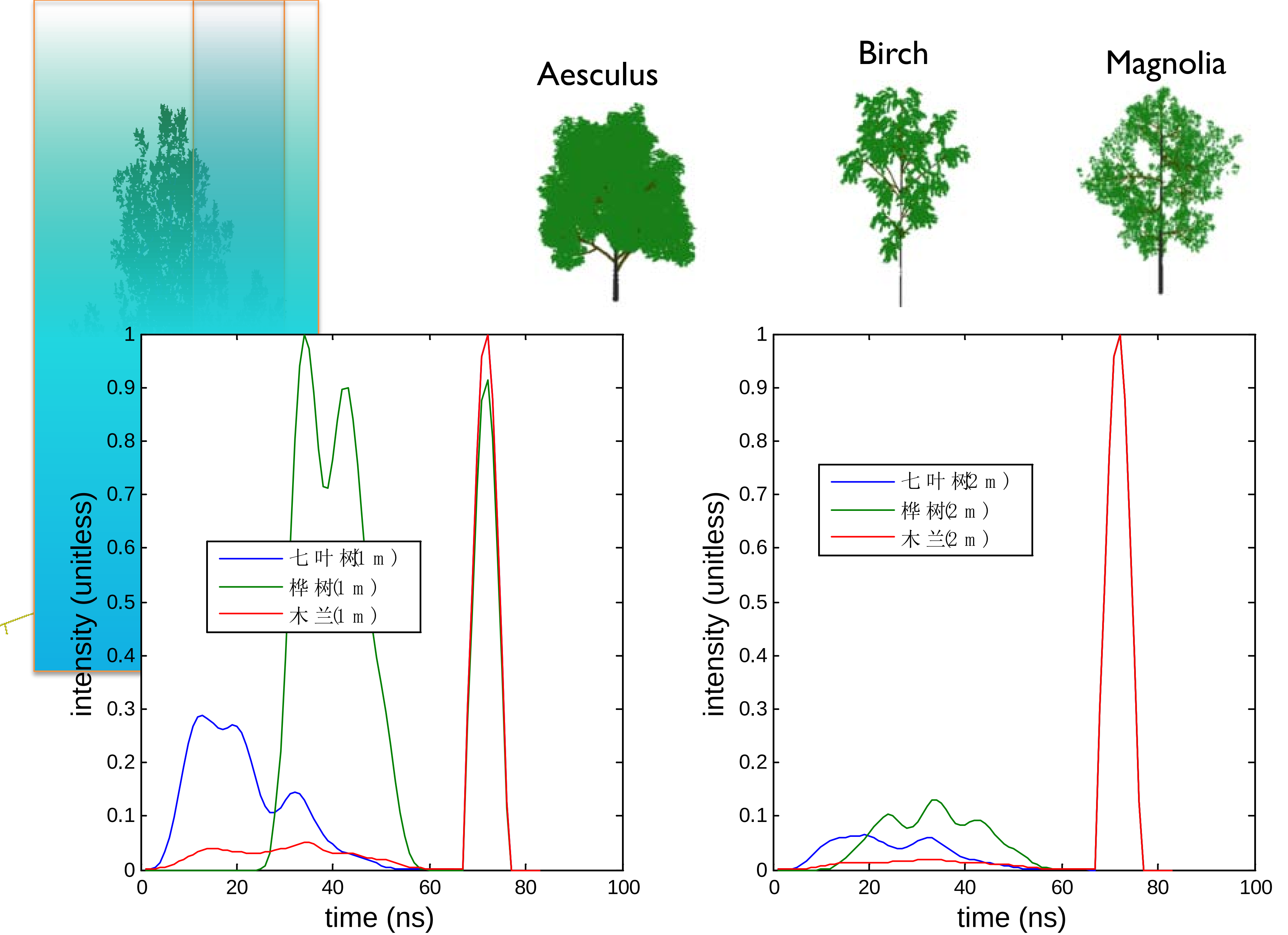

Small footprint waveform

Large scale integrated simulation
VNIR and TIR

100m by 300m

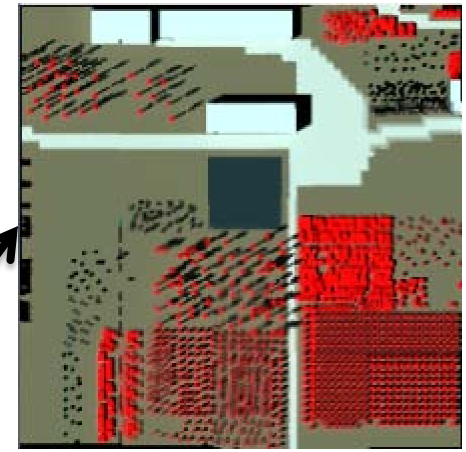

（a）假彩色影像(NIR,R,G)

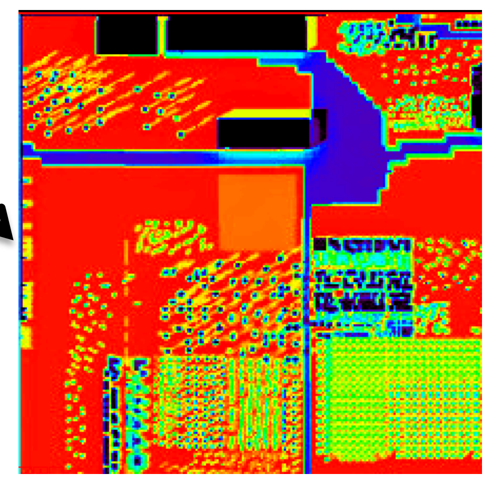

（b）伪彩色热红外(TIR)

2. Objective and motivation

- I work in BJFU, the focus is forest
- What to inverse in **forestry**
  - 2D covers: land use, tree species
  - 3D structures: DEM, Volume, Biomass
  - 4D changes: disturbance, growth

Optical data alone is not sufficient

Optical + microwave is required

Yang Zhang et al., 2015

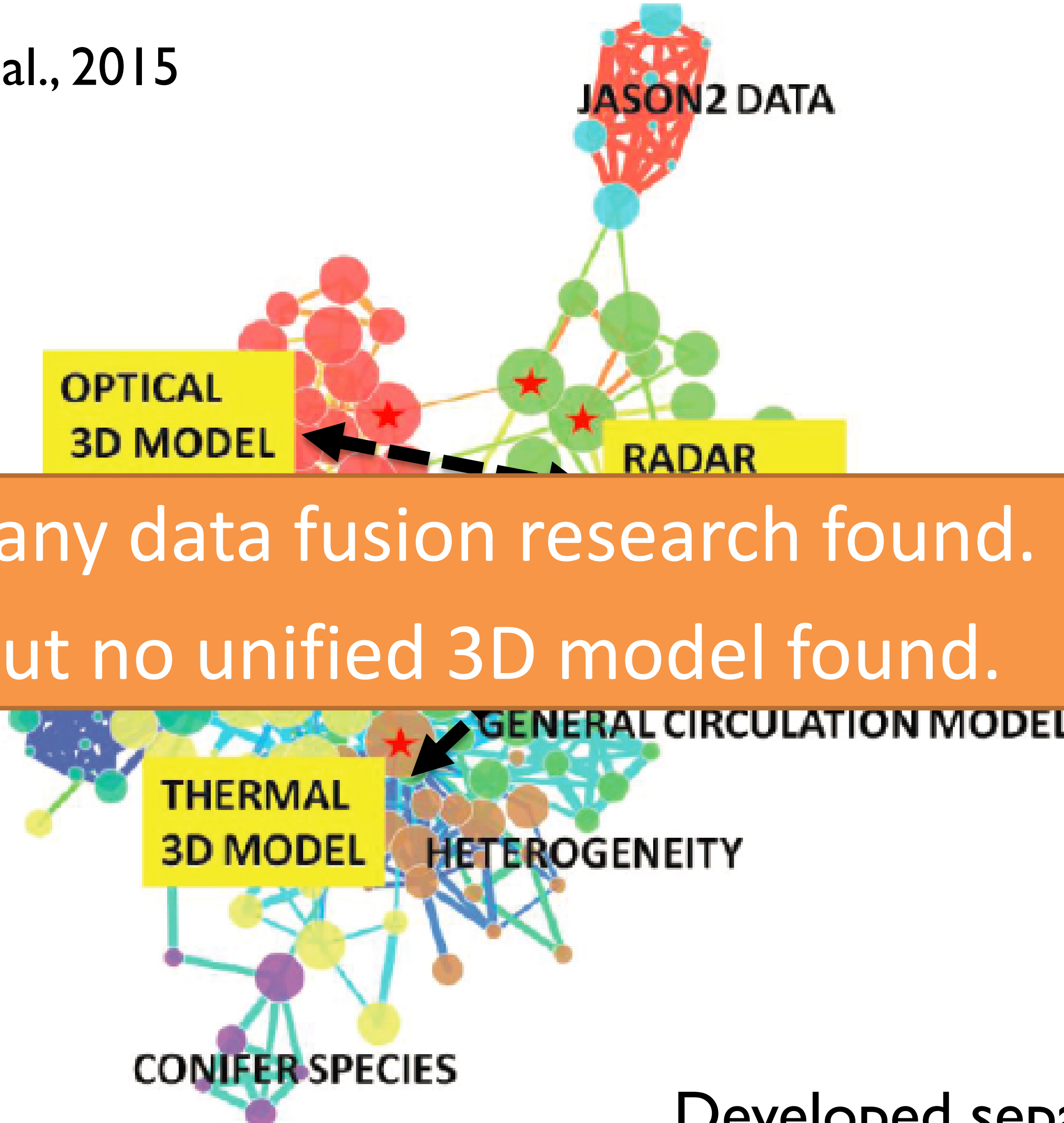

Many data fusion research found.

But no unified 3D model found.

Developed separately

2. Objective and motivation

- Why not unify the model development?
  - Wide knowledge base: fewer integrated talents
  - Different Imaging mechanism

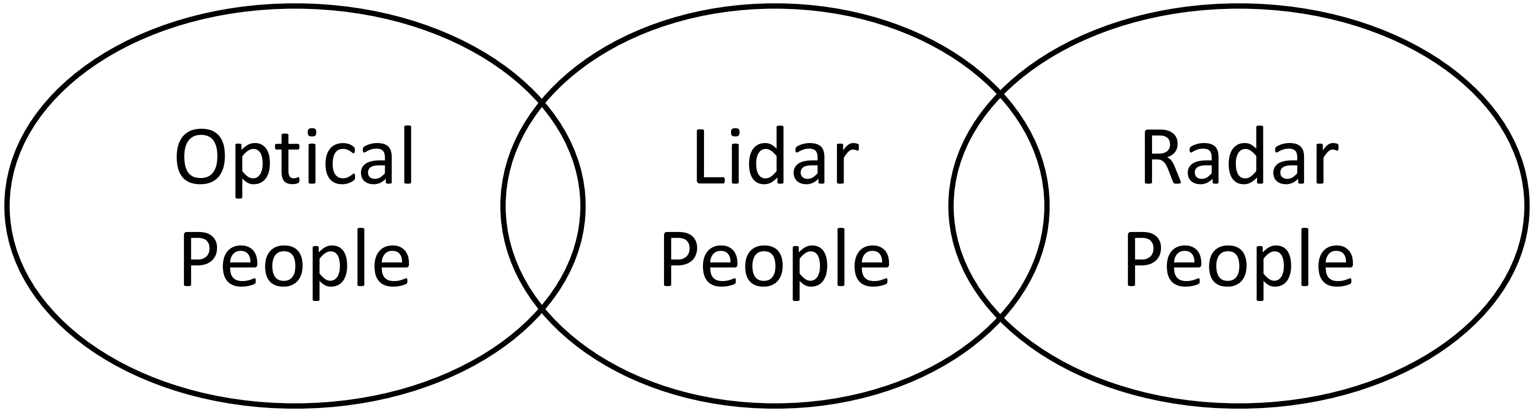

Different imaging mechanism due to wave-particle duality

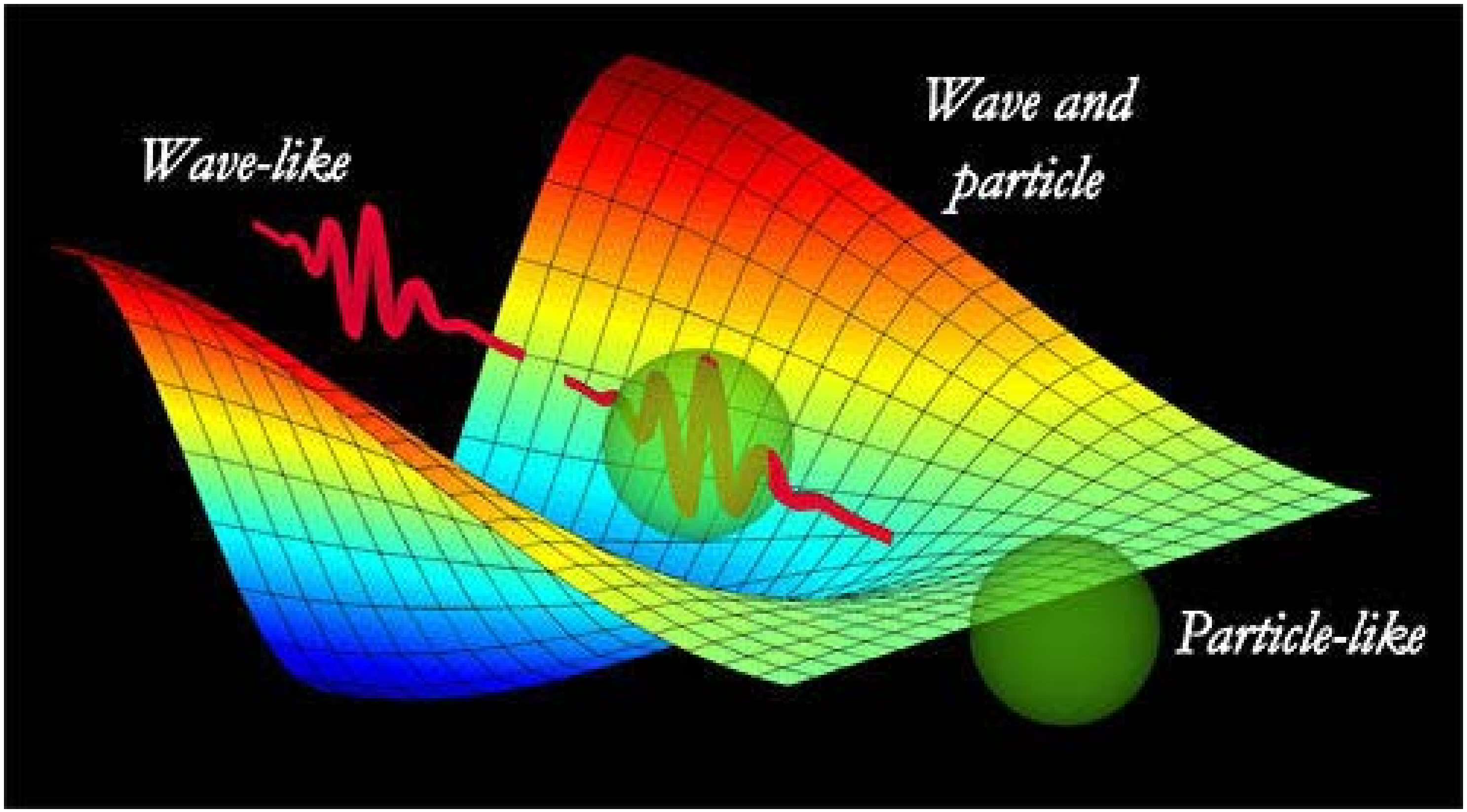

波粒二象性（Wave-particle duality）

2. Objective and motivation

- Although difficult, a unified multi-sensor simulation model will be beneficial:
  - No need to waste time finding models
  - Consistent input/output parameters
  - Easy to educate and use: 3D + Windows
  - High accuracy

3. Unification method selection
--modeling strategies for optical regions

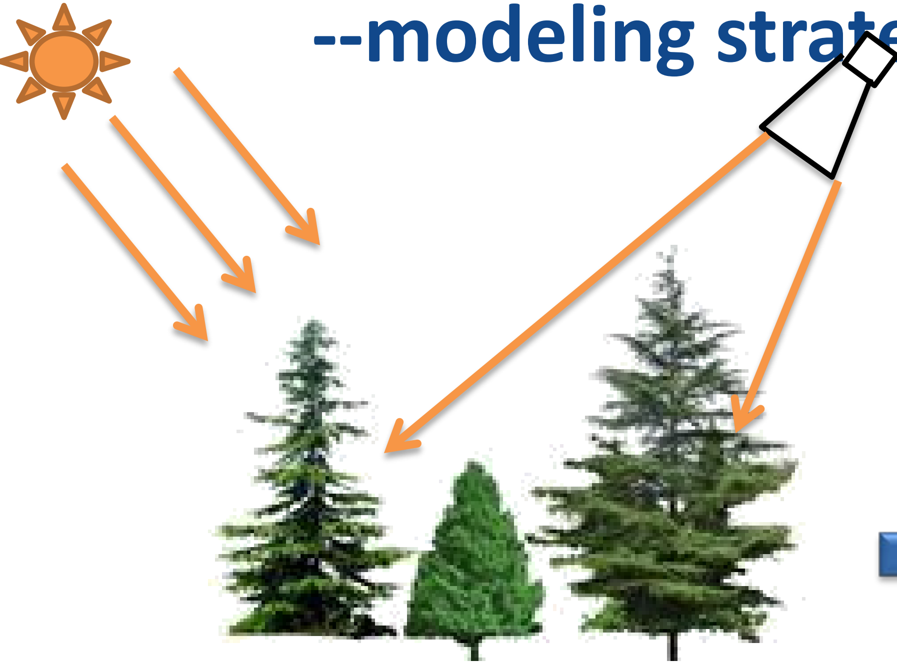

Two major factors:

- Shadows (sun or view)
- Multiple scattering

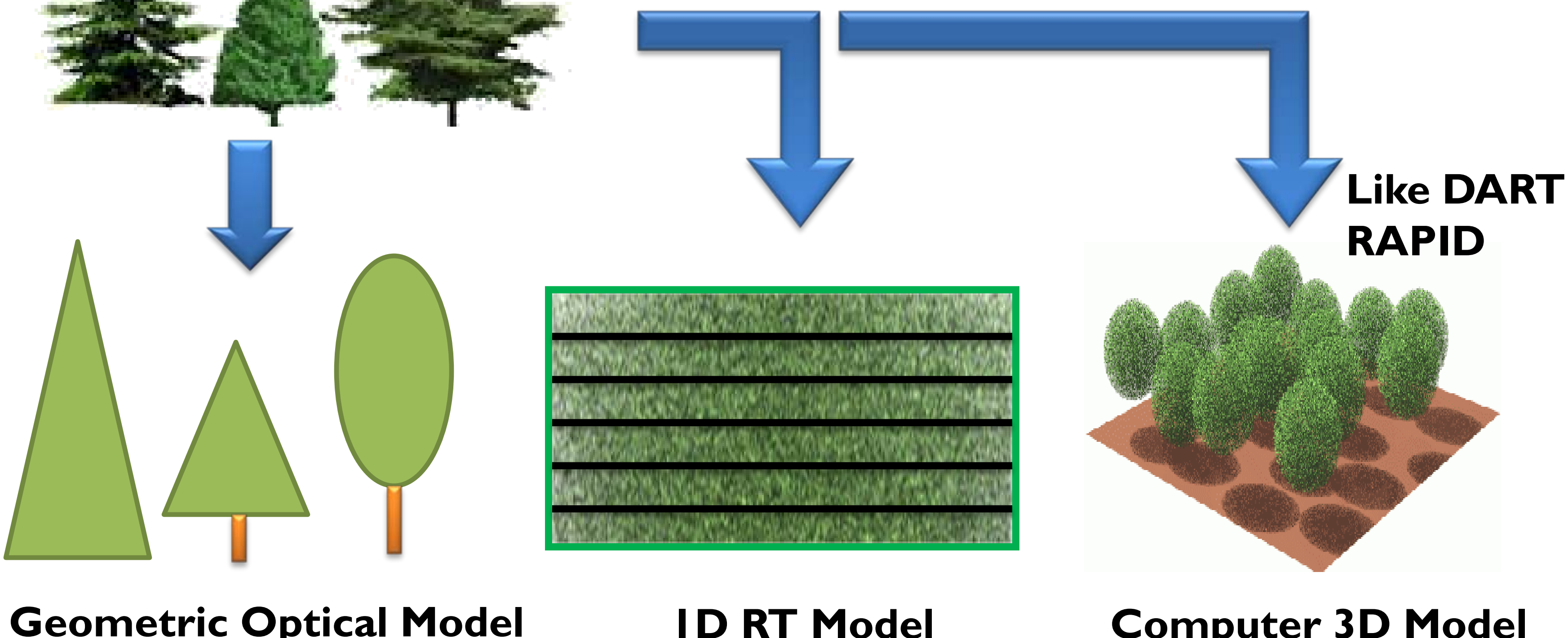

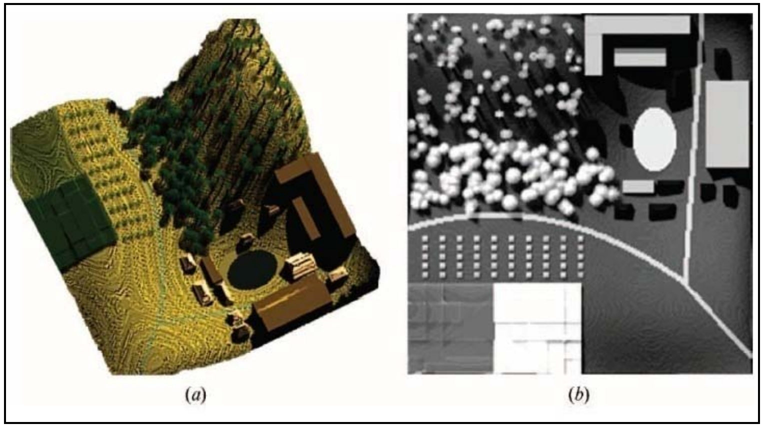

(DART model, 1996)

Ray tracing

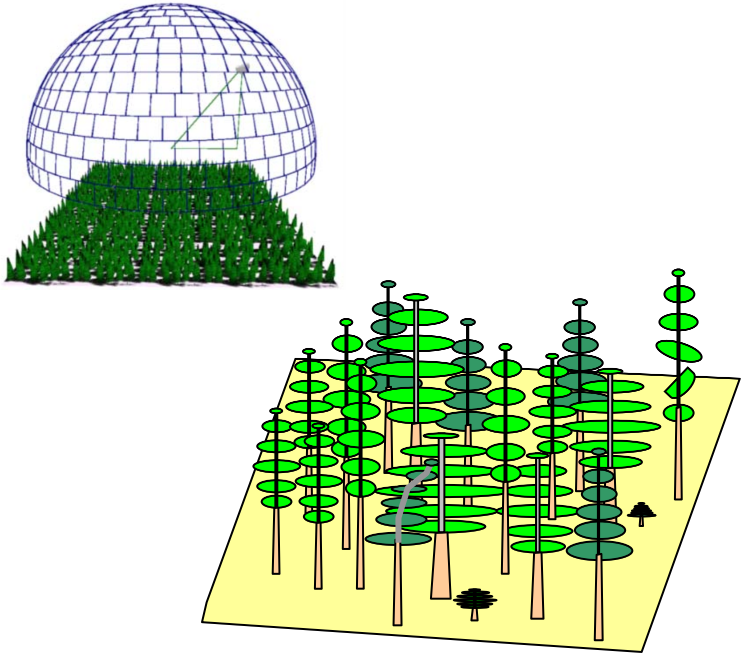

(Huang et al., 2013)

Radiosity

3. Unification method selection
--modeling strategies for Radar

Incoherent

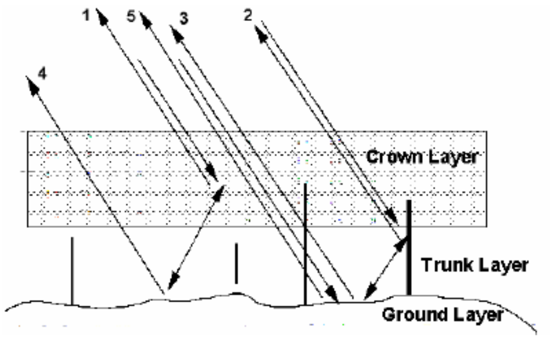

2D RT MIMICS (Ulaby, 1990)

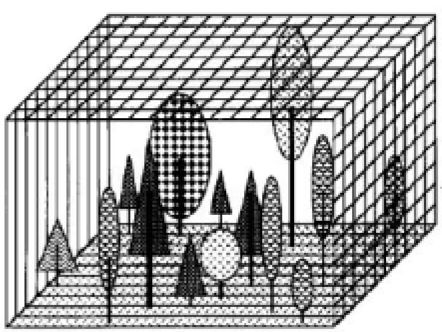

Computer 3D Model Non-coherent (SUN,1995)

Coherent

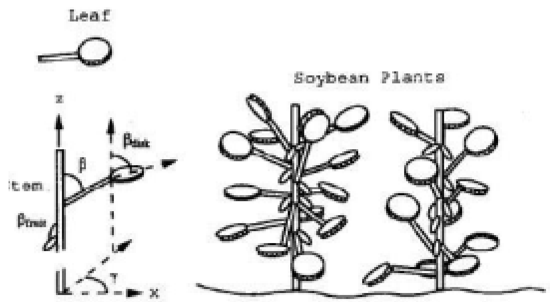

Corn Coherent Model (Yueh 1992)

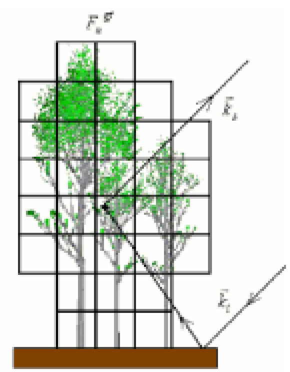

3D Coherent Model (Liu DW 2010)

Major Features:

- Vector RT
- Cohence
- Strong Specular scattering

- No shadow but with extinction
- Multiple scattering overlooked

Name: SUN model

- •Incoherent
- •Voxel structure
- •0.5 resolution
- •Double bouncing

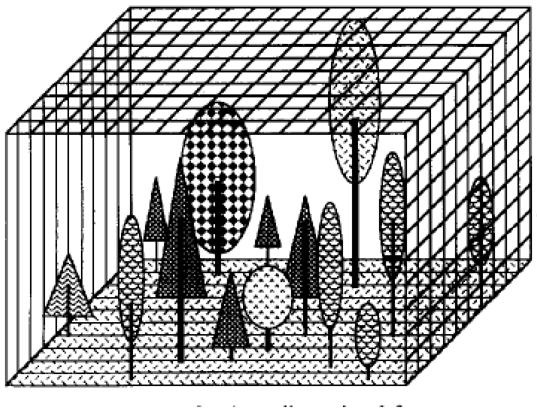

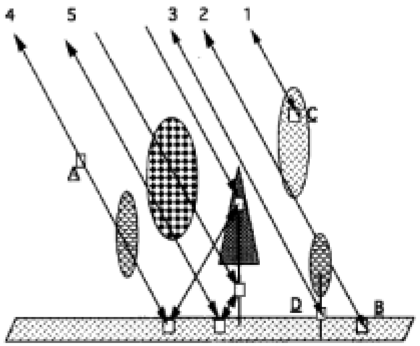

(Sun et al., 1995)

Ray tracing

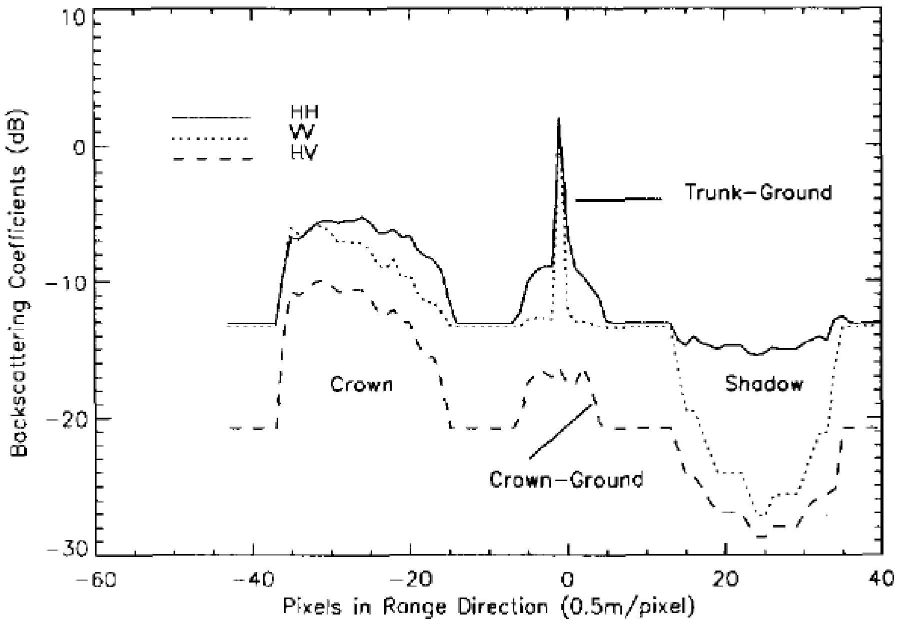

How to bridge optical and radar

- Ray tracing may be a natural choice
  - E.g. DART model + SUN model
  - The efficiency is relatively low for multiple scattering
  - Two groups of corporation
- Radiosity has special potential
  - High efficiency of multiple scattering
  - No radar application found so far
  - One group One model → **a unified model**

4. RAPID2– The unified model

- Full name:
  - Radiosity Applicable to Porous IndiviDual Object version 2 for multi-sensors
- Multi-Sensors include:
  - Optical sensors: Visible and near infrared region
  - TIR sensors: Thermal region
  - Lidar sensors: TLS, ALS and spaceborne
  - Radar sensor: X, C, L, P bands

classical radiosity equation

$$B_i = E_i + \rho_i \sum_{j=1}^{2N} F_{ij} B_j$$

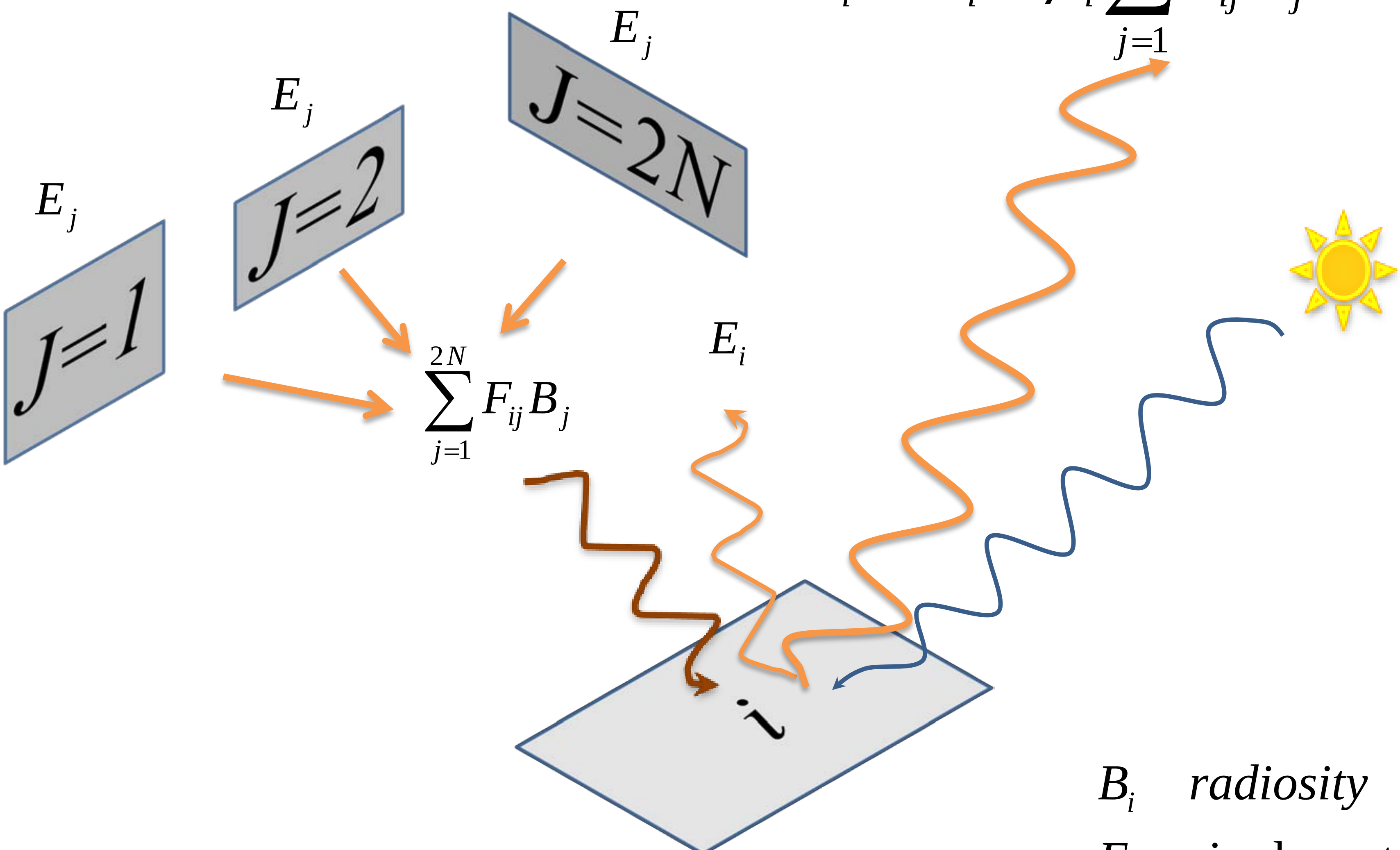

B_i *radiosity*

E_i single scattering

ρ_i *reflectivity*

What if transmittance happens?

$$B_i = E_i + \rho_i \sum_{j=1}^{2N} F_{ij} B_j + \tau_i \sum_{k=1}^{2N} F_{ij} B_j$$

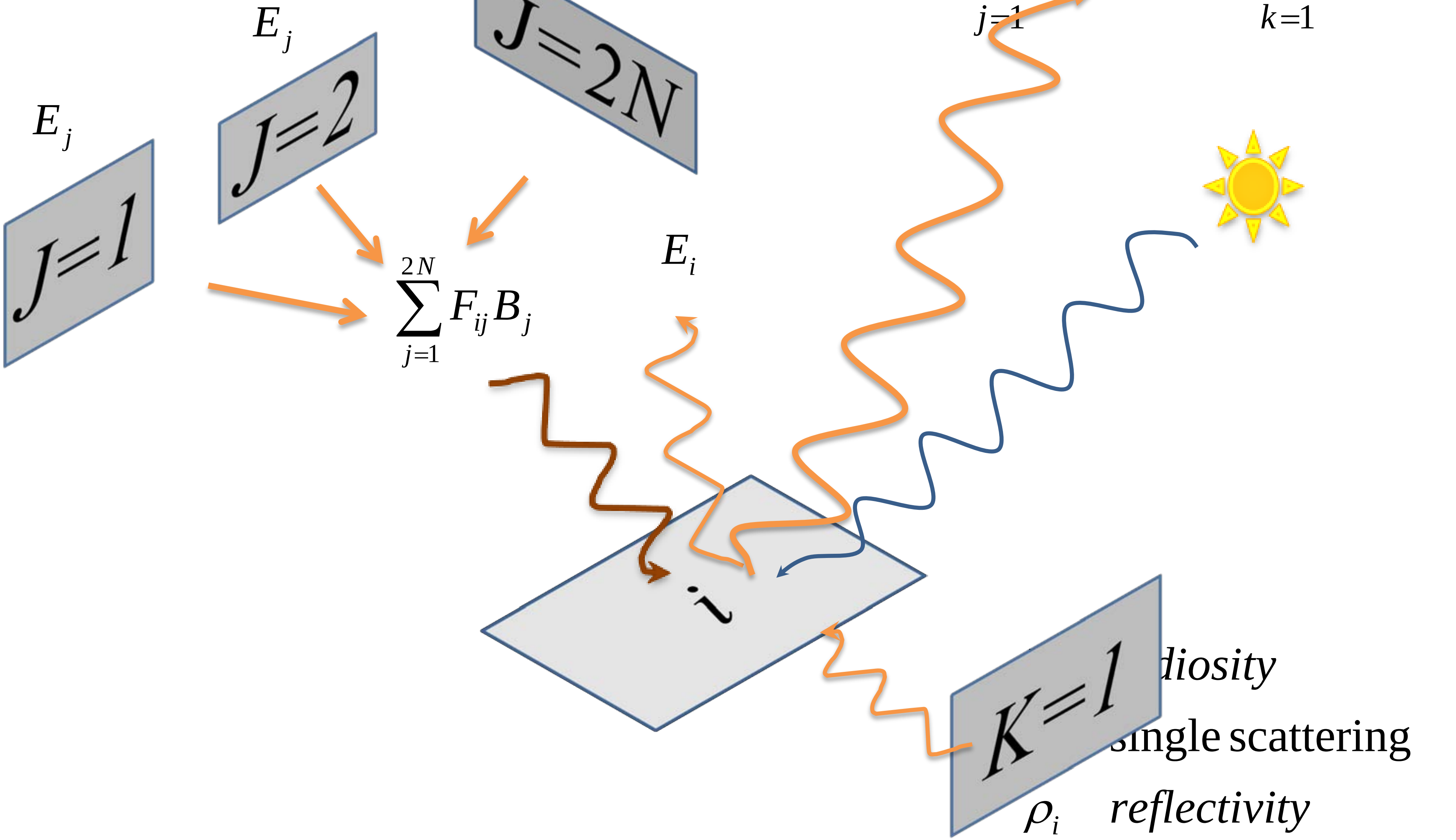

What if thermal wavelengths?

$$B_i = \varepsilon\sigma T_i^{\,4} + \rho_i \sum_{j=1}^{2N} F_{ij} B_j$$

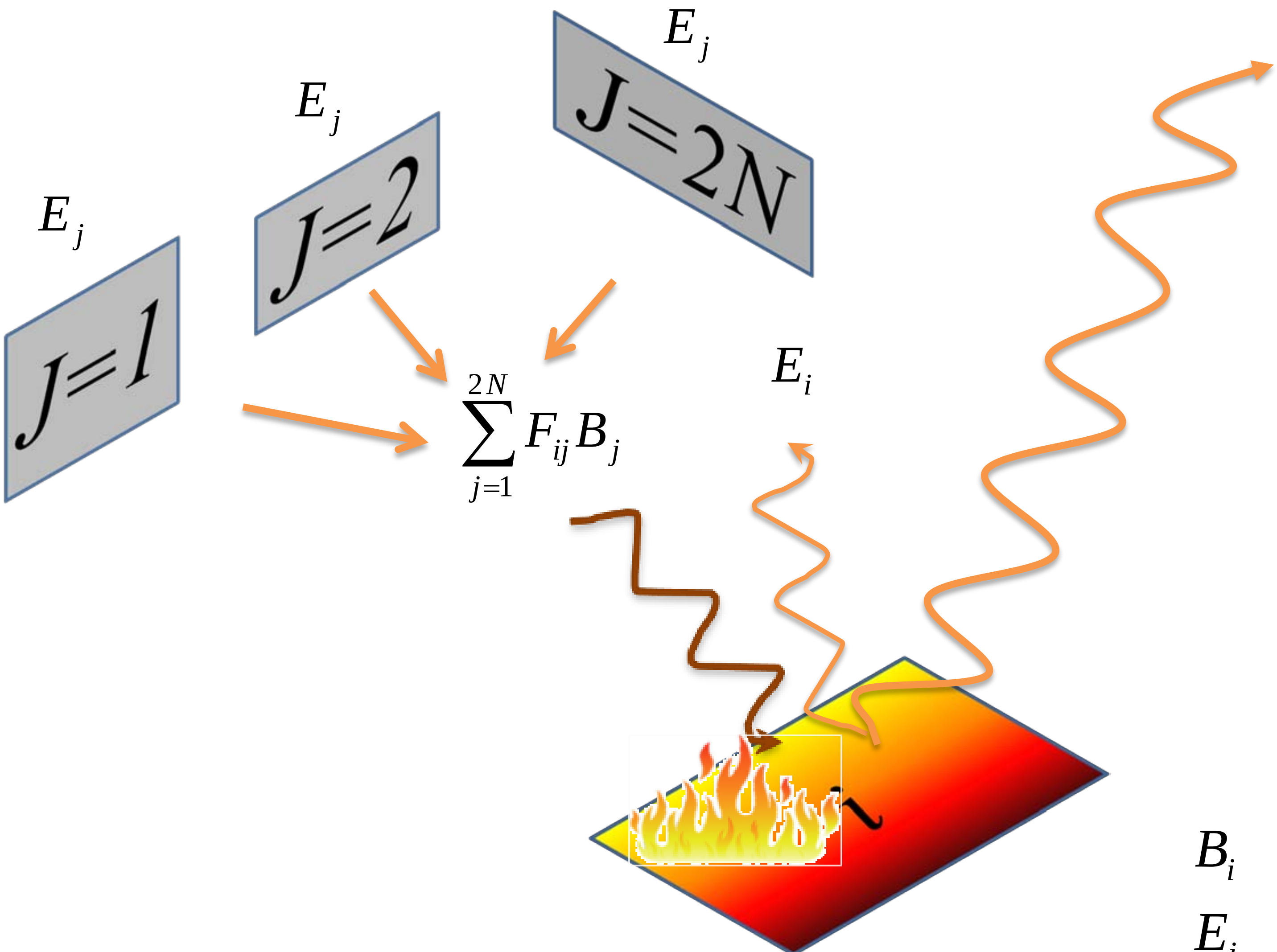

B_i *radiosity*

E_i single scattering

ρ_i *reflectivity*

What if microwave wavelengths?

$$\sigma = \frac{4\pi R^2}{A}\frac{\langle I_r \rangle}{\langle I_i \rangle}$$

$$\sigma_{db} = 10\log_{10}(\sigma)$$

New features:

- **Polarimetric**
- **Vector**

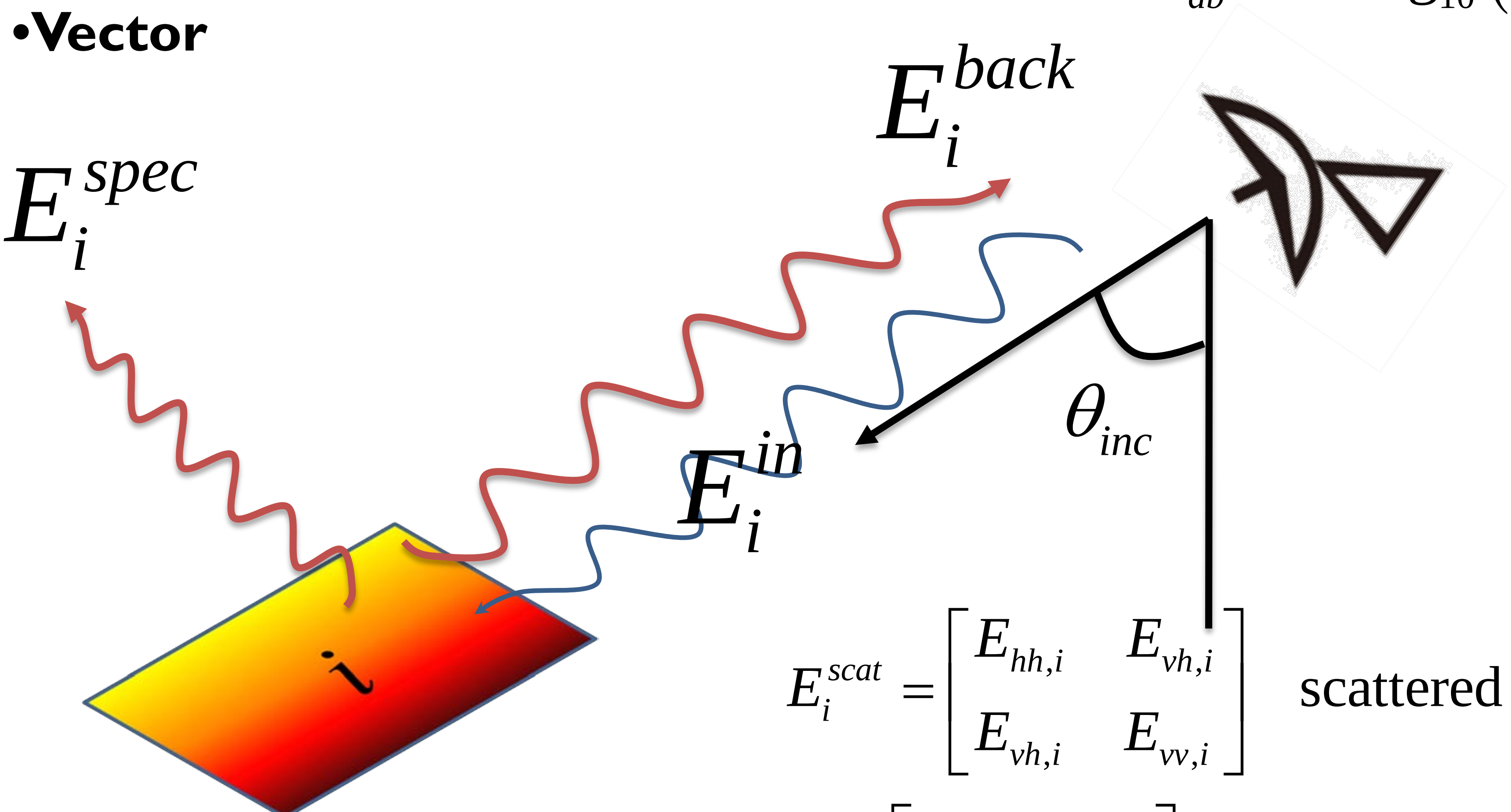

$$E_i^{scat} = \begin{bmatrix} E_{hh,i} & E_{vh,i} \\ E_{vh,i} & E_{vv,i} \end{bmatrix}$$ scattered EM

$$S_i = \begin{bmatrix} S_{hh,i} & S_{vh,i} \\ S_{vh,i} & S_{vv,i} \end{bmatrix}$$ scattering matrix

What if microwave wavelengths?

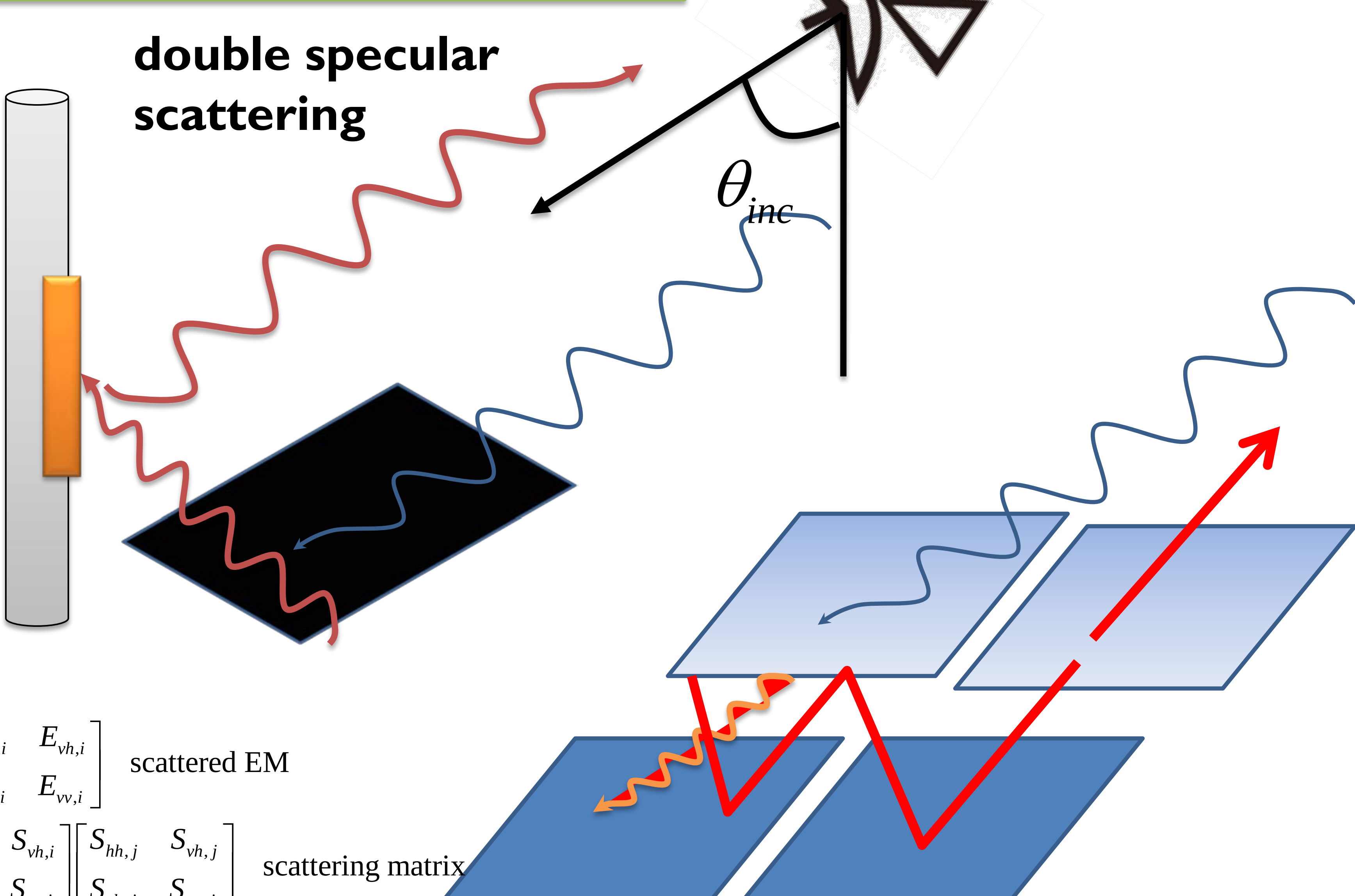

$$E_{ij}^{scat} = \begin{bmatrix} E_{hh,i} & E_{vh,i} \\ E_{vh,i} & E_{vv,i} \end{bmatrix}$$ scattered EM

$$S_{ij} = \begin{bmatrix} S_{hh,i} & S_{vh,i} \\ S_{vh,i} & S_{vv,i} \end{bmatrix} \begin{bmatrix} S_{hh,j} & S_{vh,j} \\ S_{vh,j} & S_{vv,j} \end{bmatrix}$$ scattering matrix

4. Developing the unified model RAPID2
--3D Scene description

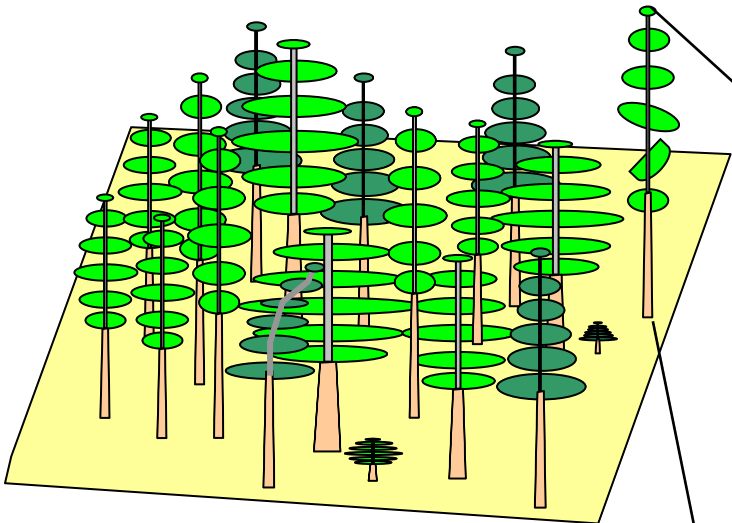

Each plant is shaped by a few polygons or non-vertical (mostly horizontal) porous thin objects.

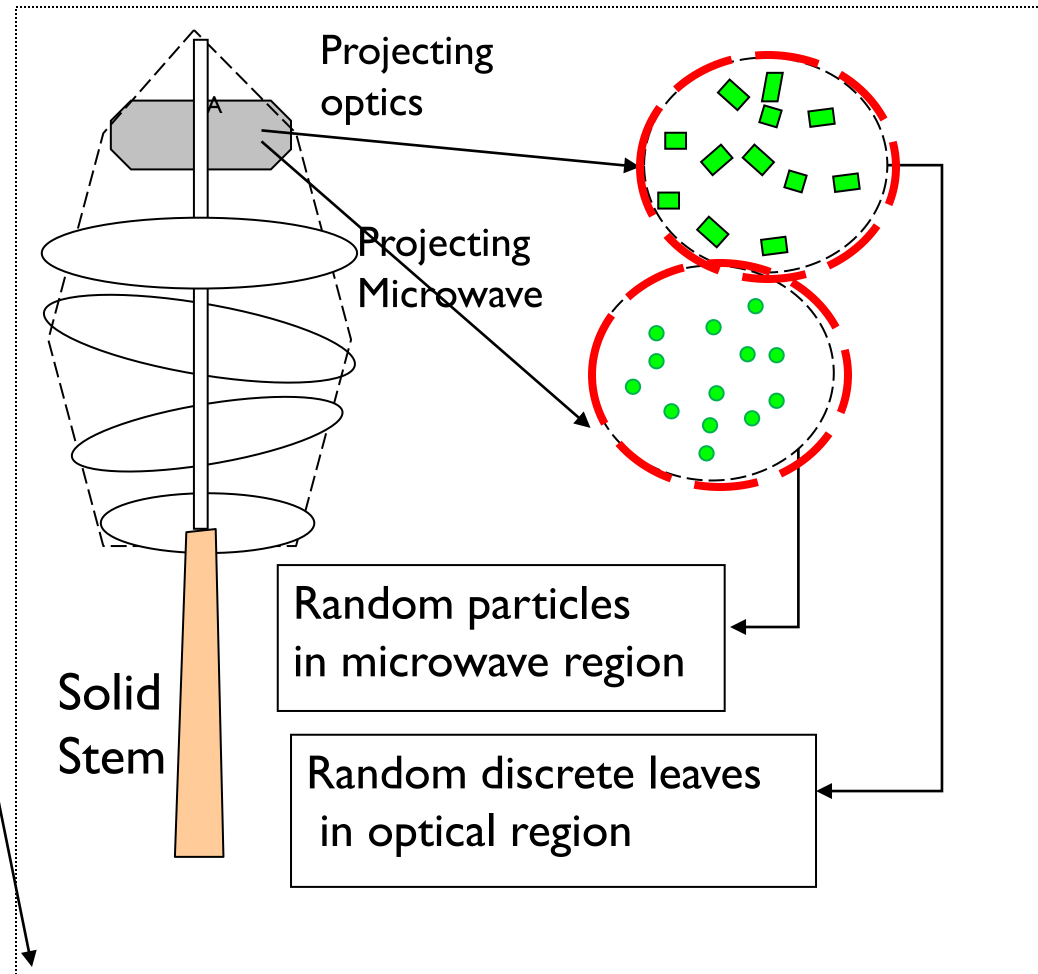

4. RAPID2
-- unified radiosity model

Radiosity for porous objects was proposed, including:

(1) Dynamic projection for porous objects

(2) Optical or scattering properties

(3) Form factor determination

(4) Radiosity solution

(5) BRF, sigma and returns

(4.1) dynamic projection

When wavelength is far less than leaf size
Specific random leaves are generated during projection

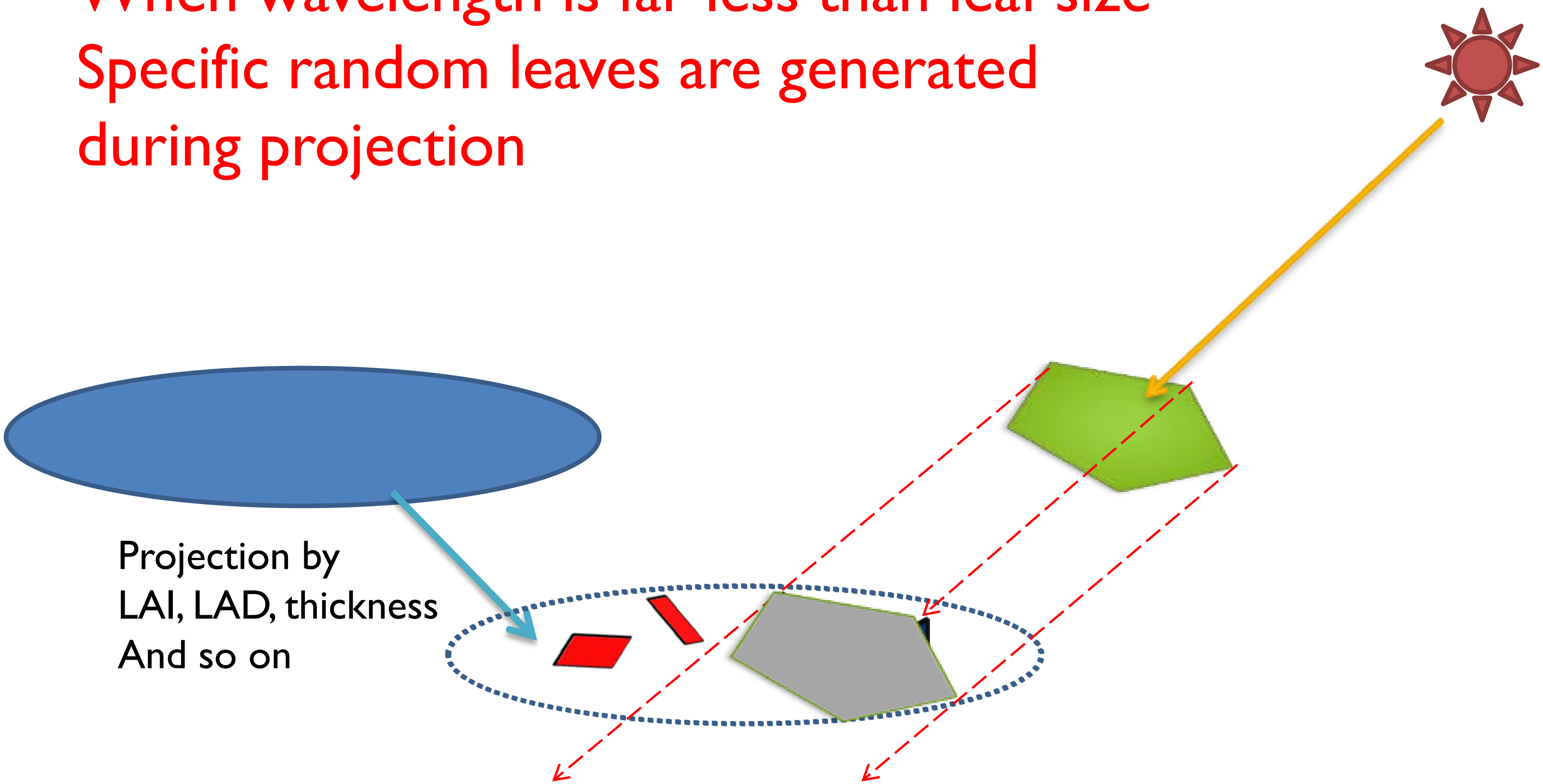

When wavelength is comparable to or larger than leaf size
Random pixels are generated during projection
Which means no significant shadows

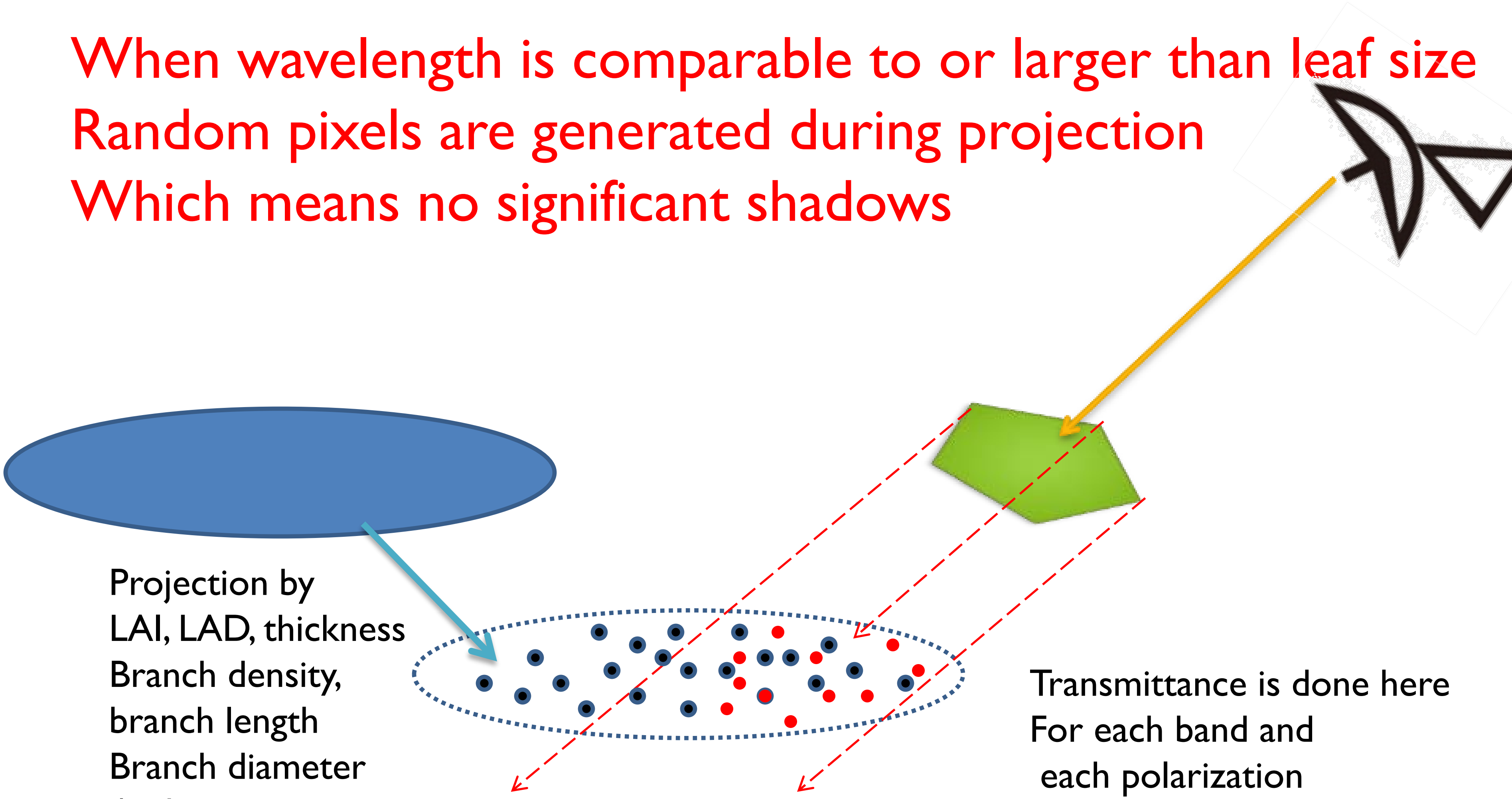

The pixel density is based on
the extinction coefficients

(4.2.1) For optical properties

How much for Upside

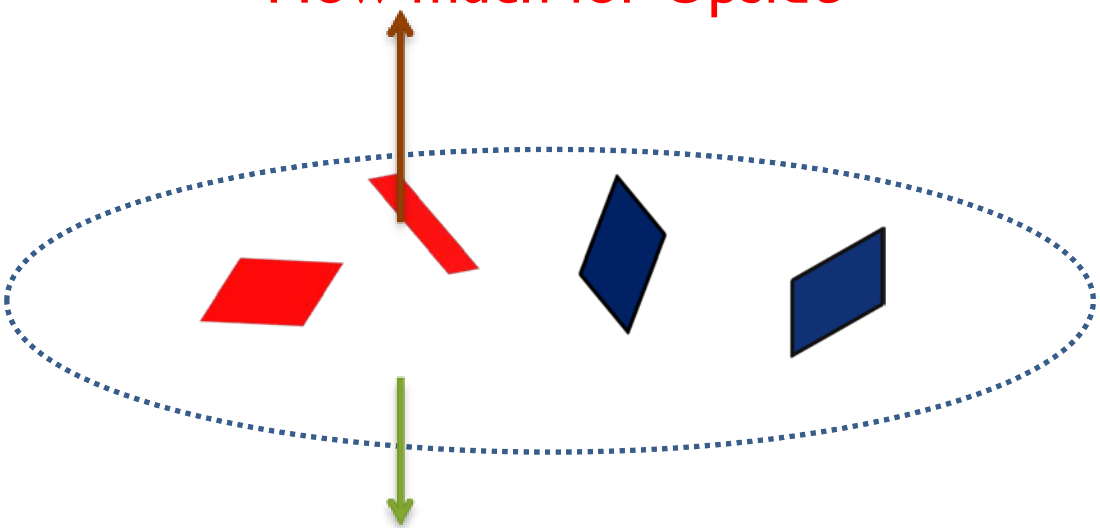

How much for downside

$$Mean[\frac{(1+\cos\theta)}{2}]$$

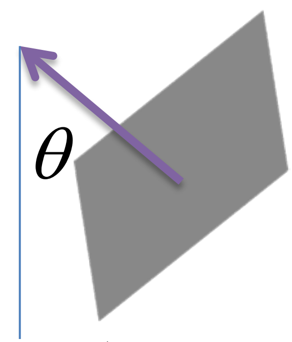

$$Mean[\frac{(1-\cos\theta)}{2}]$$

$$\hat{\rho}_{SN} = 0.5(\rho_{SN}+\tau_{SN}) + 0.5(\rho_{SN}-\tau_{SN})\frac{1}{SSM}\sum_{j=1}^{SSM}\cos^2\theta_j$$

$$\hat{\tau}_{SN} = 0.5(\rho_{SN}+\tau_{SN}) + 0.5(\tau_{SN}-\rho_{SN})\frac{1}{SSM}\sum_{j=1}^{SSM}\cos^2\theta_j$$

(4.2.2) For microwave scattering properties

Averaging the scattering matrix of elements (leaf or branch) within the porous object

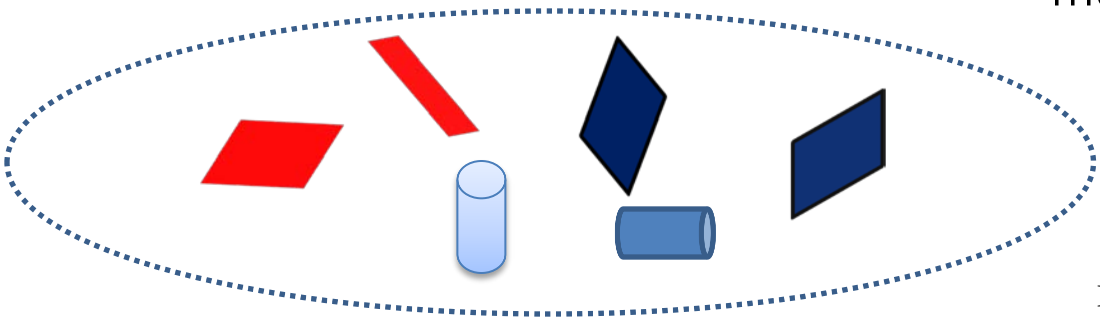

$$S_i = \begin{bmatrix} \langle S_{hh,i} \rangle & \langle S_{vh,i} \rangle \\ \langle S_{vh,i} \rangle & \langle S_{vv,i} \rangle \end{bmatrix}$$

Single Leaf model

Senior, T. B. A., K. Sarabandi, and F. T. Ulaby, "Measuring and Modeling the Backscattering Cross Section of a Leaf," *Radio Science, Vol. 22, No. 6,* November, 1987, pp. 1109-1116.

Single Cylinder model:

Karam, M. A. and A. K. Fung, "Electromagnetic Scattering from a Layer of Finite Length, Randomly Oriented, Dielectric, Circular Cylinders Over a Rough Interface with Application to Vegetation," *Internationa1 Journal of Remote Sensing, Vol. 9, No. 6, June 1988, pp. 1109-1134.*

Scattering matrix: 2 by 2 Complex values → 4 by 4 real values

$$P = \begin{bmatrix} |S_{vv}|^2 & |S_{vh}|^2 & \mathrm{Re}\left(S_{vh}^* S_{vv}\right) & -\mathrm{Im}\left(S_{vh}^* S_{vv}\right) \\ |S_{hv}|^2 & |S_{hh}|^2 & \mathrm{Re}\left(S_{hh}^* S_{hv}\right) & -\mathrm{Im}\left(S_{hh}^* S_{hv}\right) \\ 2\,\mathrm{Re}\left(S_{vv} S_{hv}^*\right) & 2\,\mathrm{Re}\left(S_{vh} S_{hh}^*\right) & \mathrm{Re}\left(S_{vv} S_{hh}^* + S_{vh} S_{hv}^*\right) & -\mathrm{Im}\left(S_{vv} S_{hh}^* - S_{vh} S_{hv}^*\right) \\ 2\,\mathrm{Im}\left(S_{vv} S_{hv}^*\right) & 2\,\mathrm{Im}\left(S_{vh} S_{hh}^*\right) & \mathrm{Im}\left(S_{vv} S_{hh}^* + S_{vh} S_{hv}^*\right) & \mathrm{Re}\left(S_{vv} S_{hh}^* - S_{vh} S_{hv}^*\right) \end{bmatrix}$$

$$L_{i,0}\left(\Omega_{back}\right) = \begin{bmatrix} I_v^S \\ I_h^S \\ U^S \\ V^S \end{bmatrix} = P\left(\Omega_{in};\Omega_{back}\right) \begin{bmatrix} T_v & 0 & 0 & 0 \\ 0 & T_h & 0 & 0 \\ 0 & 0 & 1 & 0 \\ 0 & 0 & 0 & 1 \end{bmatrix} \begin{bmatrix} I_v^{in} \\ I_h^{in} \\ U^{in} \\ V^{in} \end{bmatrix}$$

polarization extension of the backward radiance

(4.3.1) Form factor in optical region

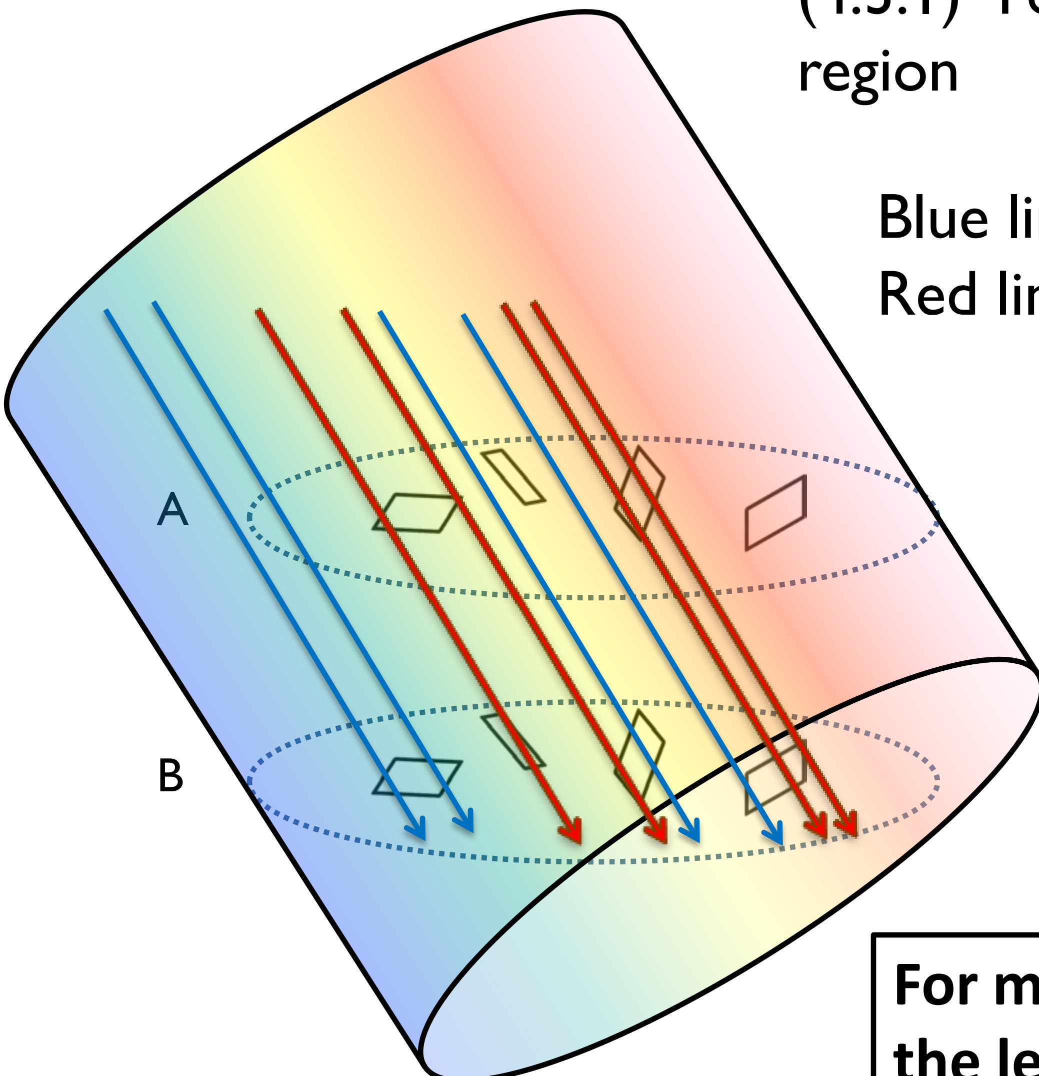

Blue lines: no overlapping rays Nb
Red lines: overlapped rays Nr

At a reasonable ray resolution, form factor is the average value of
Nr/(Nr + Nb)
at all directions

For microwave,
the leaves are changed to pixels

(4.3.2) Form factor in microwave

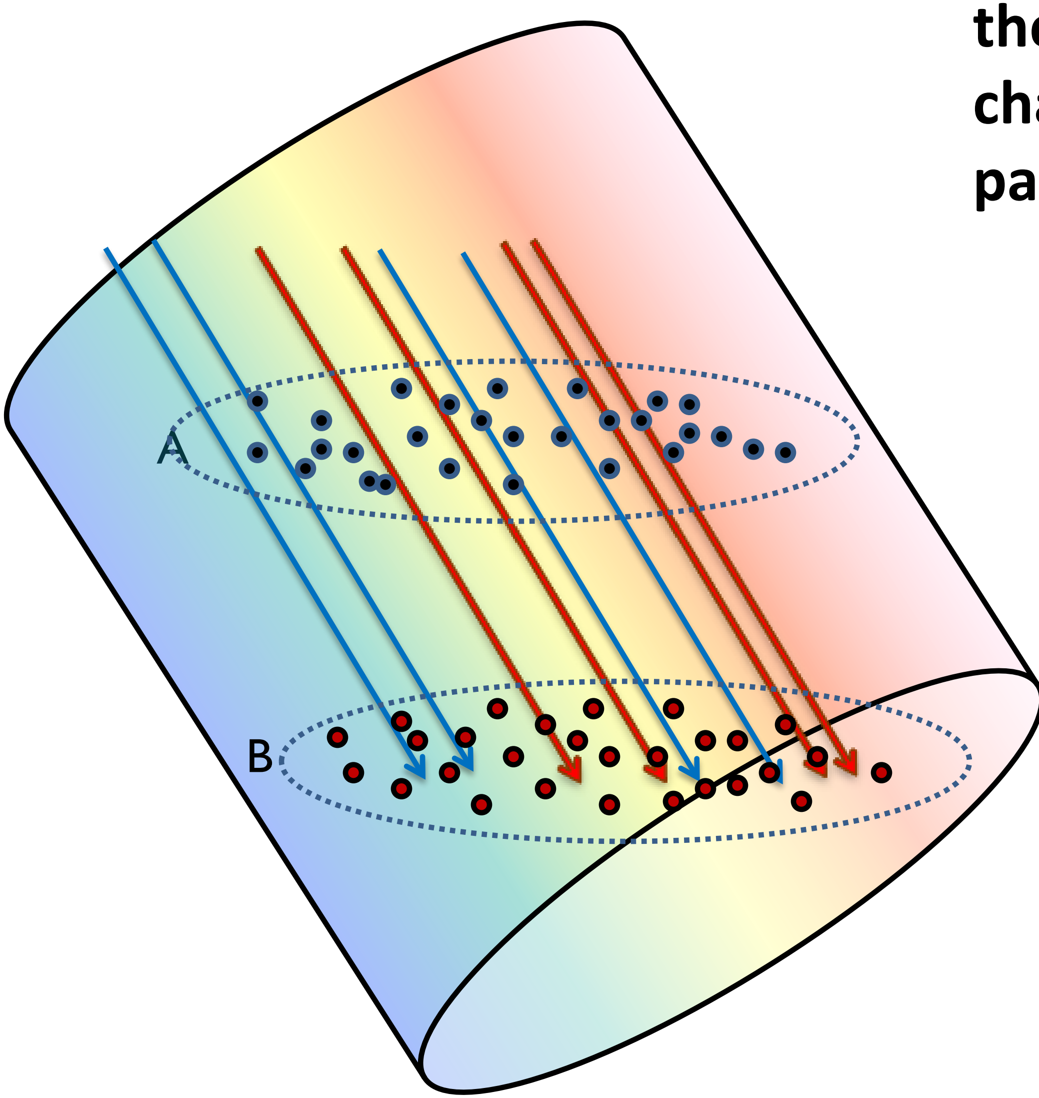

the leaves or branches are changed to pixels or particles

Four form factors:
- **Spec-spec**
- **Spec-dif**
- **Dif-spec**
- **Dif-dif**

Form factors are estimated as:

→intersection fractions from two directions

→incident direction and its mirror direction

$$F_{ij,dif-dif} = F_{ij,dif-spec} = F_{ij}$$

$$F_{ij,spec-spec} = F_{ij,spec-dif} = \pi F_{ij} \times \left| dot\left(\Omega_{spec}, \Omega_{ij}\right) \right|$$

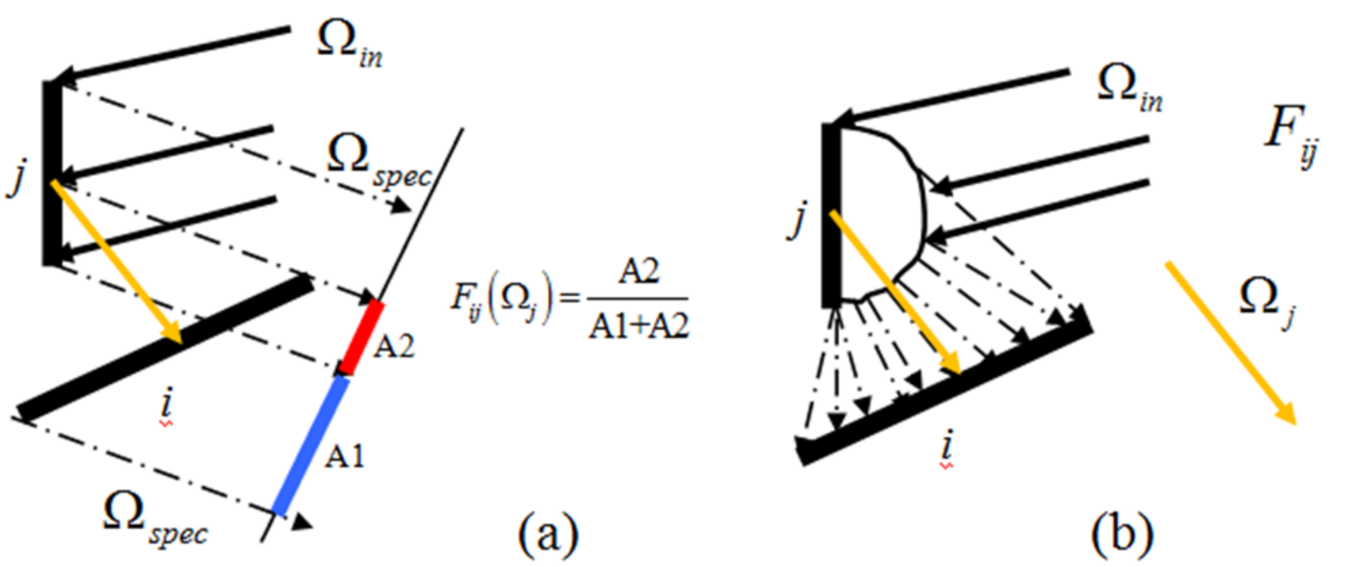

Figure 3. Extended view factors: (a) scattering from a specular object j; (b) scattering from a diffuse object j.

(4.4) Radiosity solution:

In optical region, it is important to separate sunlit part from mean value of a porous object

$$B_{i,shd} = E_{i,shd} + \rho_i \sum_j F_{ij} B_j + \tau_i \sum_k F_{ik} B_k$$

$$B_{i,lit} = E_{i,lit} + \rho_i \sum_j F_{ij} B_j + \tau_i \sum_k F_{ik} B_k$$

In microwave region, it is not necessarily to separate sunlit part because of hot spot effects

But need to separate specular and diffuse scattering

$$B_i = \boxed{B_{i,spec}} + \boxed{B_{i,dif}} = \begin{bmatrix} B_{vv,i} & B_{vh,i} \\ B_{hv,i} & B_{hh,i} \end{bmatrix}$$

Specular double bouncing radiosity

$$B_{i,spec}\left(\Omega_{back}\right) = \sum_{j=1}^{n_j}\left(E^1_{ij,spec-spec} + E^1_{ij,dif-spec}\right) \times T_i\left(\Omega_{back}\right)$$

Diffuse radiosity with multiple scattering

$$B_{i,dif} = E^0_{i,back} \times T_i\left(\Omega_{back}\right) + \sum_{j=1}^{n_j} B_{j,dif} \times F_{ij,dif-dif} \times S_i \times T_i\left(\Omega_{back}\right)$$

(4.5.1) BRF (bidirectional reflectance factor)

$$BRF(v) = \frac{\sum_{i=1}^{N} \left[B_{i,lit} A_{i,lit}(v) + B_{i,shd} A_{i,shd}(v) \right]}{\sum_{i=1}^{N} \left[A_{i,lit}(v) + A_{i,shd}(v) \right]}$$

- A is the area of lit or shaded part;
- Affine projection equations were used to determine which leaf is sunlit or shaded.

(4.5.2) BCS (backscattering cross section)

8 scattering sources

$$M_{tot} = M_c + M_t + M_g + M_{g-c} + M_{c-g} + M_{g-t} + M_{t-g} + M_{c-c}$$

crown

trunk

ground

Ground-crown

Crown-Ground

Ground-trunk

Trunk-ground

Crown-crow

$$\sigma_{pq}\left(\Omega_{in}\right) = \frac{4\pi \times \mu \times M_{tot}^{pq}}{\sum_{i=1}^{N} A_i(\Omega_{in}) \times T_{qq,i}}$$

- A is the area of projection size in pixel unit; T is transmittance

5. Validation

--- Comparison between RAPID2 and MIMICS

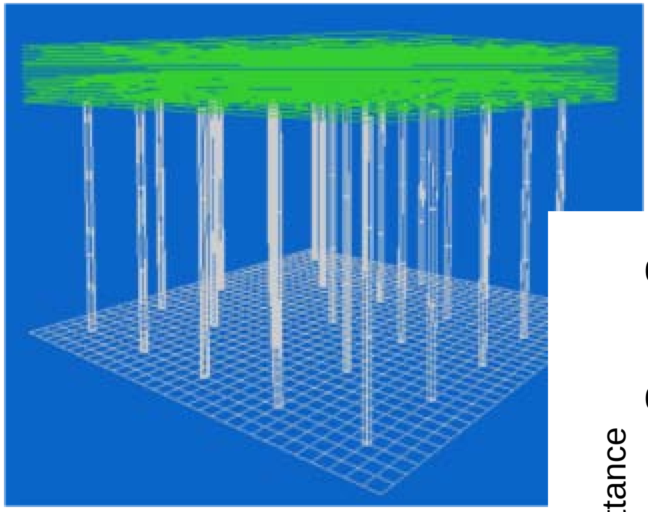

Test Scene:
8m trunk + 2m crown
LAI = 5.0
Trunk diameter: 24 cm

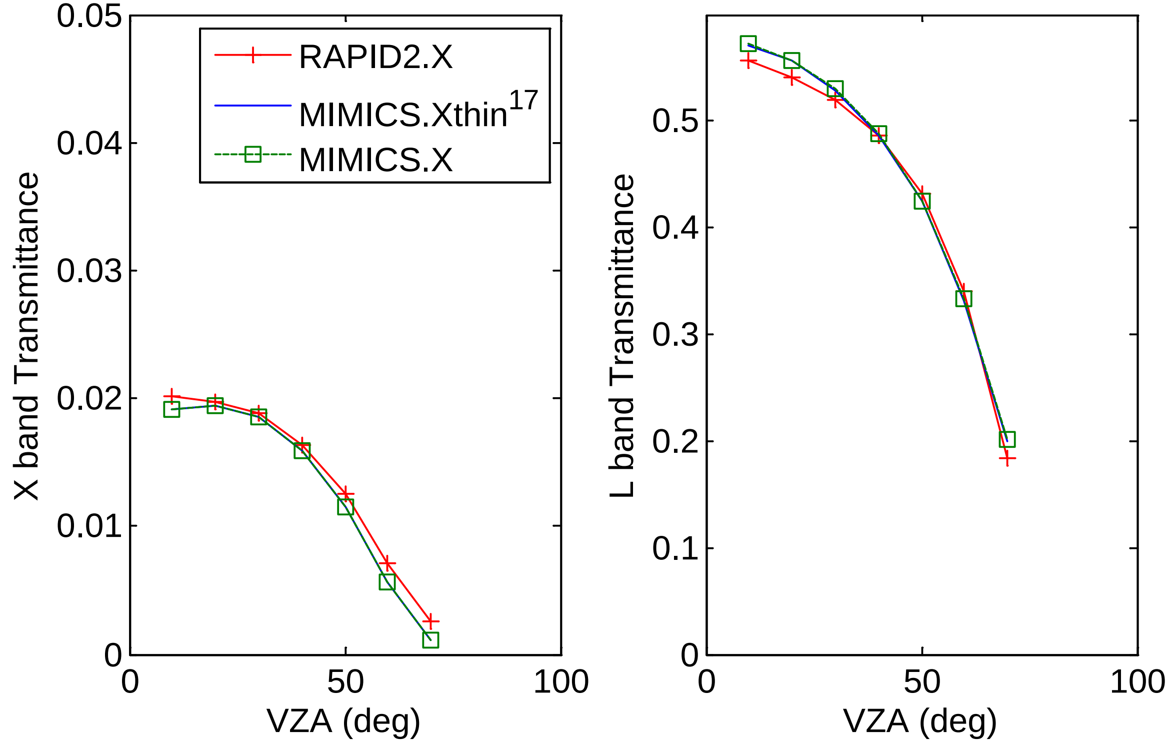

Comparing crown transmittance: (a) HH, (b) VV

To demonstrate the efficiency of dynamic projection method

5. Validation
---use AIRSAR at one mixed forest plot

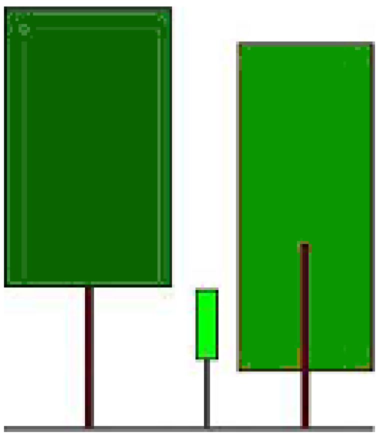

Relative tree size

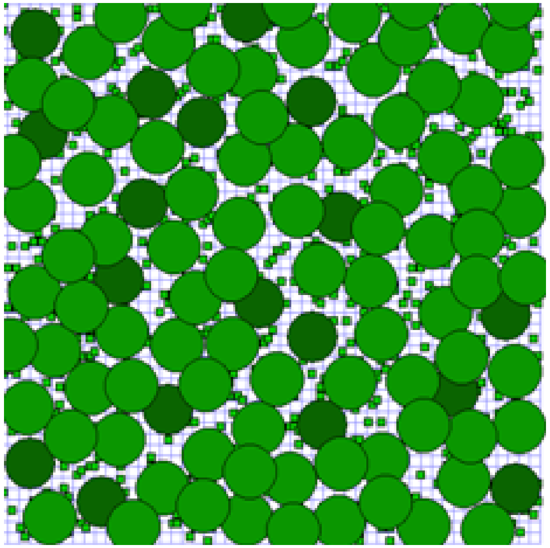

2D scenes of RAPID2

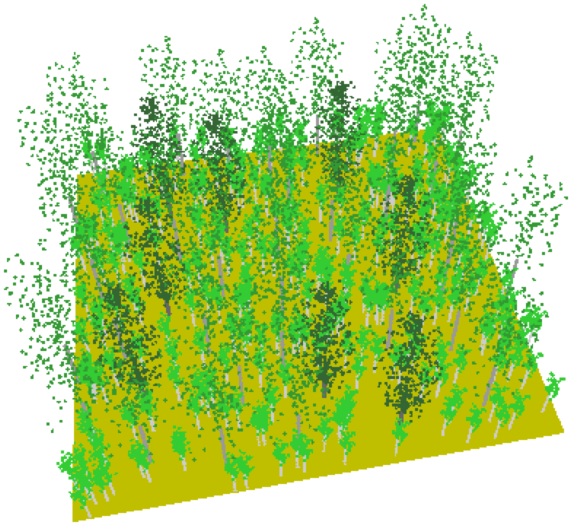

3D scenes of RAPID2

Plot 111-12 (two layers of mixed species)
White Cypress Pine (CP)
Silver-leaved ironbark (SLI)
Injune (25° 32"S, 147° 32"E), Australia (Lucas et al. 2004).

The component dielectric constants in plot 111-12

Tree classes	Band	soil	trunk	Branch	Foliage
White Cypress	C	2 – j 1	18 – j 2	18 – j 2	18 – j 4
Pine (CP)	L	2 – j 0.5	20 – j 2	20 – j 2	20 – j 4
	P	3 – j 1	25 – j 2	25 – j 2	25 – j 4
Silver-leaved	C	2 – j 1	12 – j 2	12 – j 2	12 – j 1
ironbark (SLI)	L	2 – j 0.5	25 – j 2	15 – j 2	25 – j 4
	P	3 – j 1	25 – j 2	25 – j 2	25 – j 4

JPL AIRSAR data for validation

- Date: September 2000
- Three bands: C (6 cm wavelength, 5.288 GHz), L-band (25 cm wavelength, 1.238 GHz) and P-band (68 cm, 0.428 GHz)
- Three polarizations (HH, VV and HV)
- Calibration accuracy of 1 dB

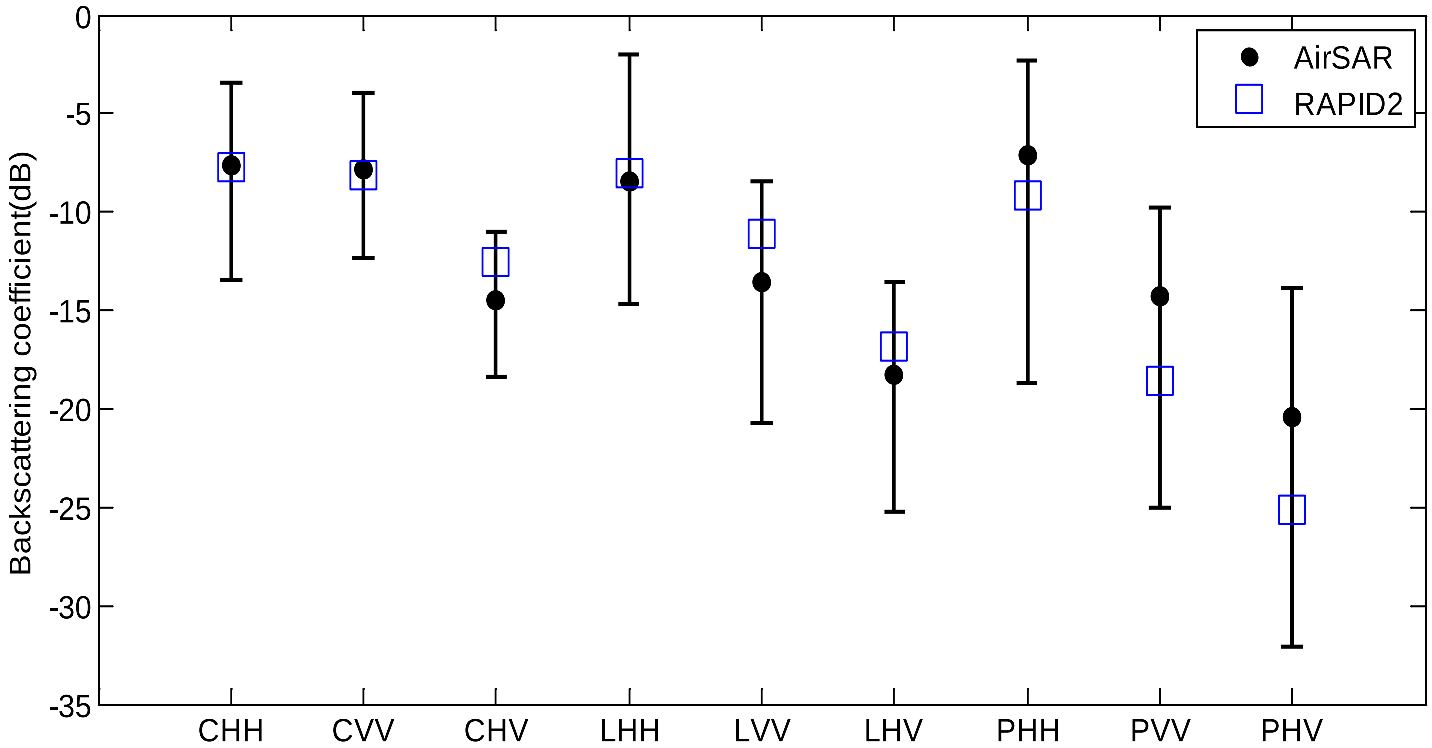

Comparison between AIRSAR-measured (mean values plus error bars) and RAPID2-simulated (square marks) backscattering coefficients for P111-12. X-axis shows for C-, L-, and P-bands at HH, VV, and HV polarizations.

5. Validation
---use AIRSAR at row-structured forests

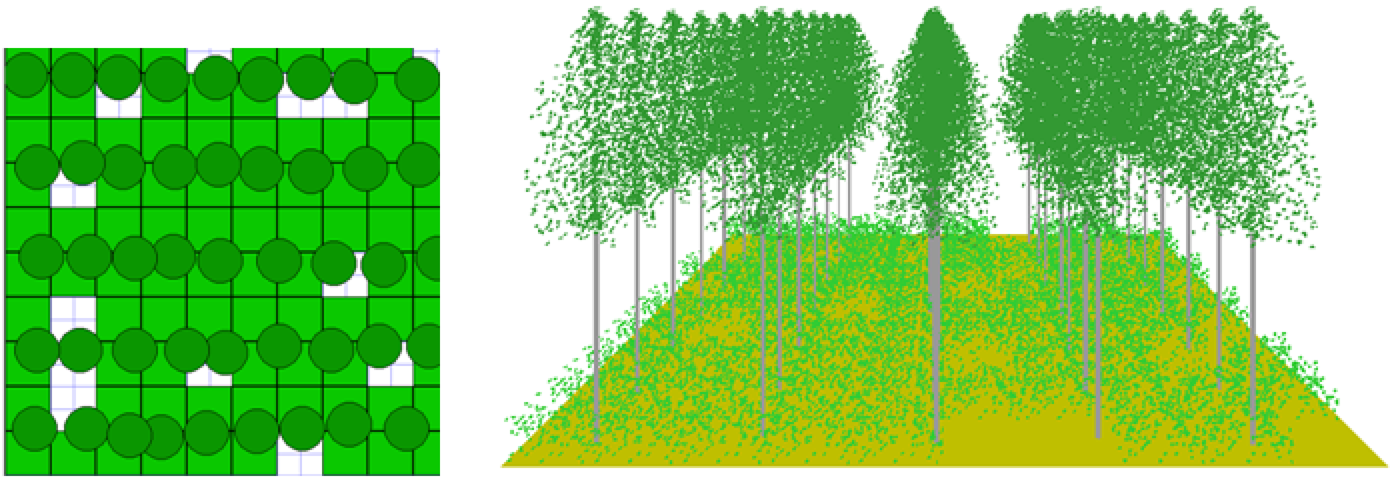

Figure 6. Schematic view of the RAPID2 scene of the row-structured maritime pine (4m row spacing) with 1 m understory

a pine plantation forest in south-western France (25° 32"S, 147° 32"E).
The forest is mainly formed of *Pinus pinaster* (Karam et al. 1995)

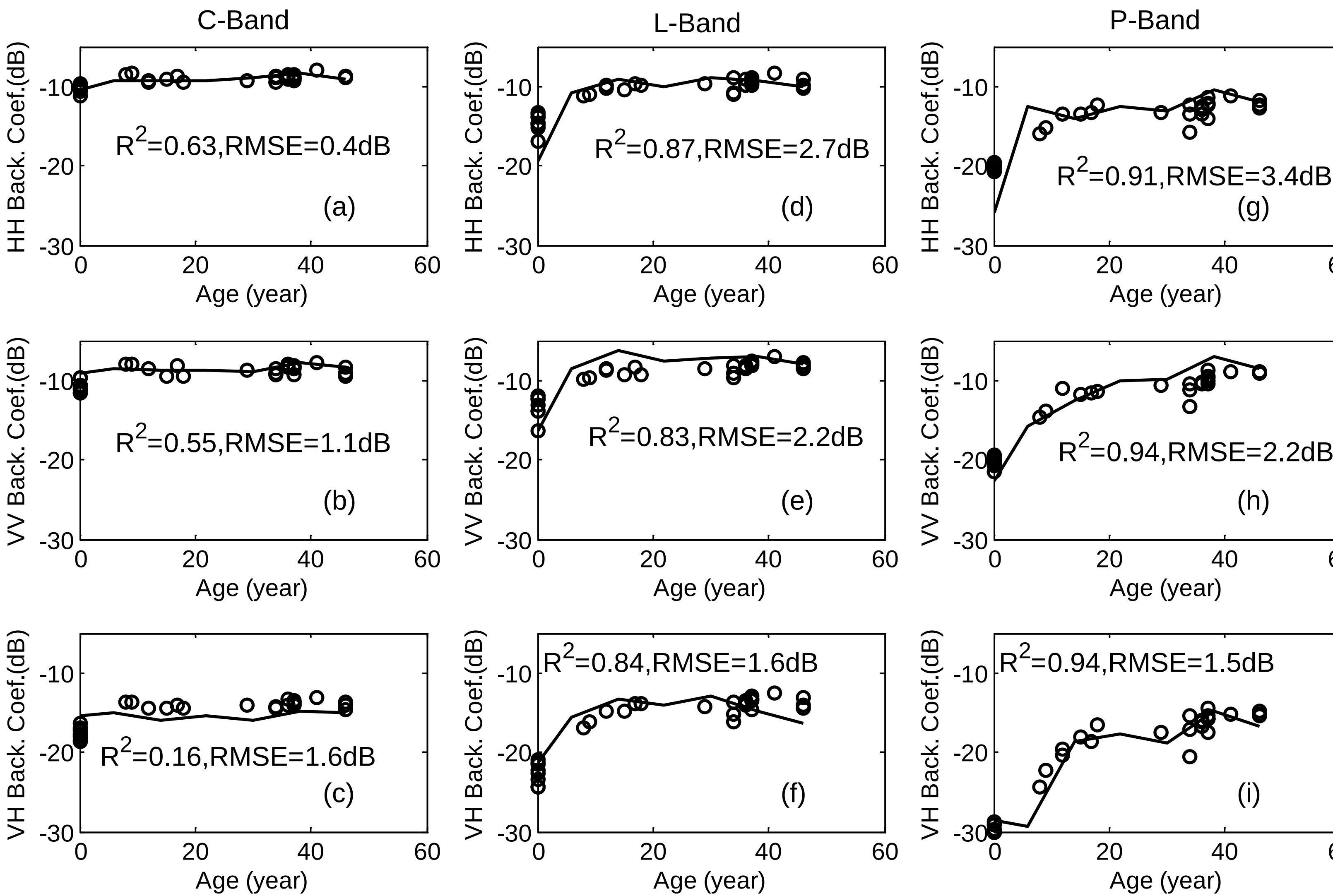

Figure 7. Simulated backscattering coefficients of RAPID2 (solid lines) and compared with AIRSAR data (dots) versus total biomass at C-, L-, and P-band.

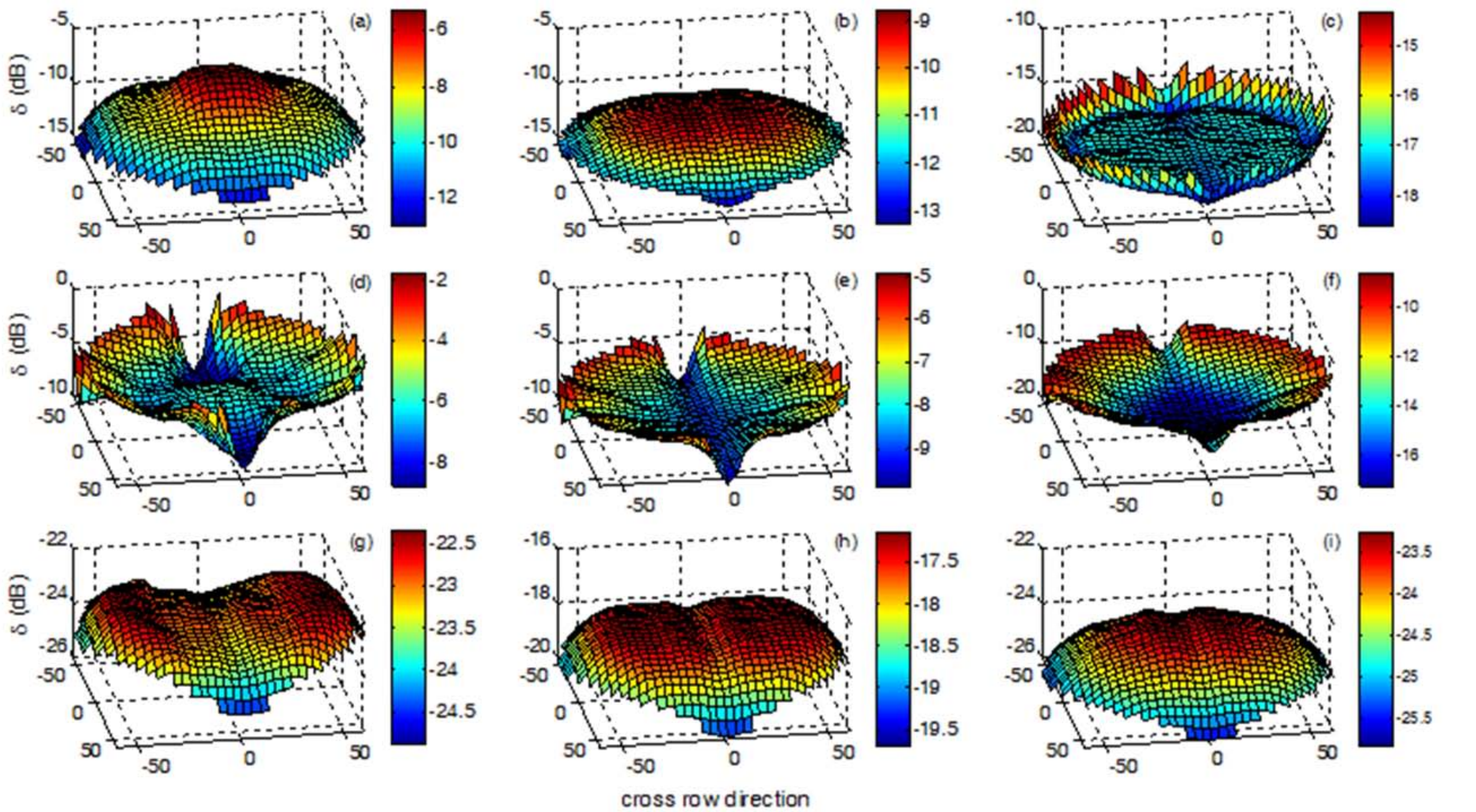

Figure 11. BCS varying with zenith and azimuth angle; band from left to right is C, L, and P band respectively; polarization from top to bottom is VV, HH, and HV respectively.

Row structure has effect on BCS

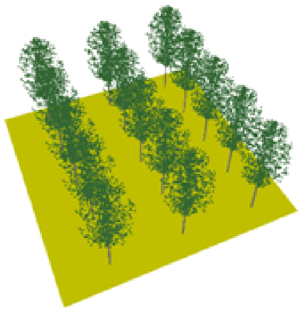

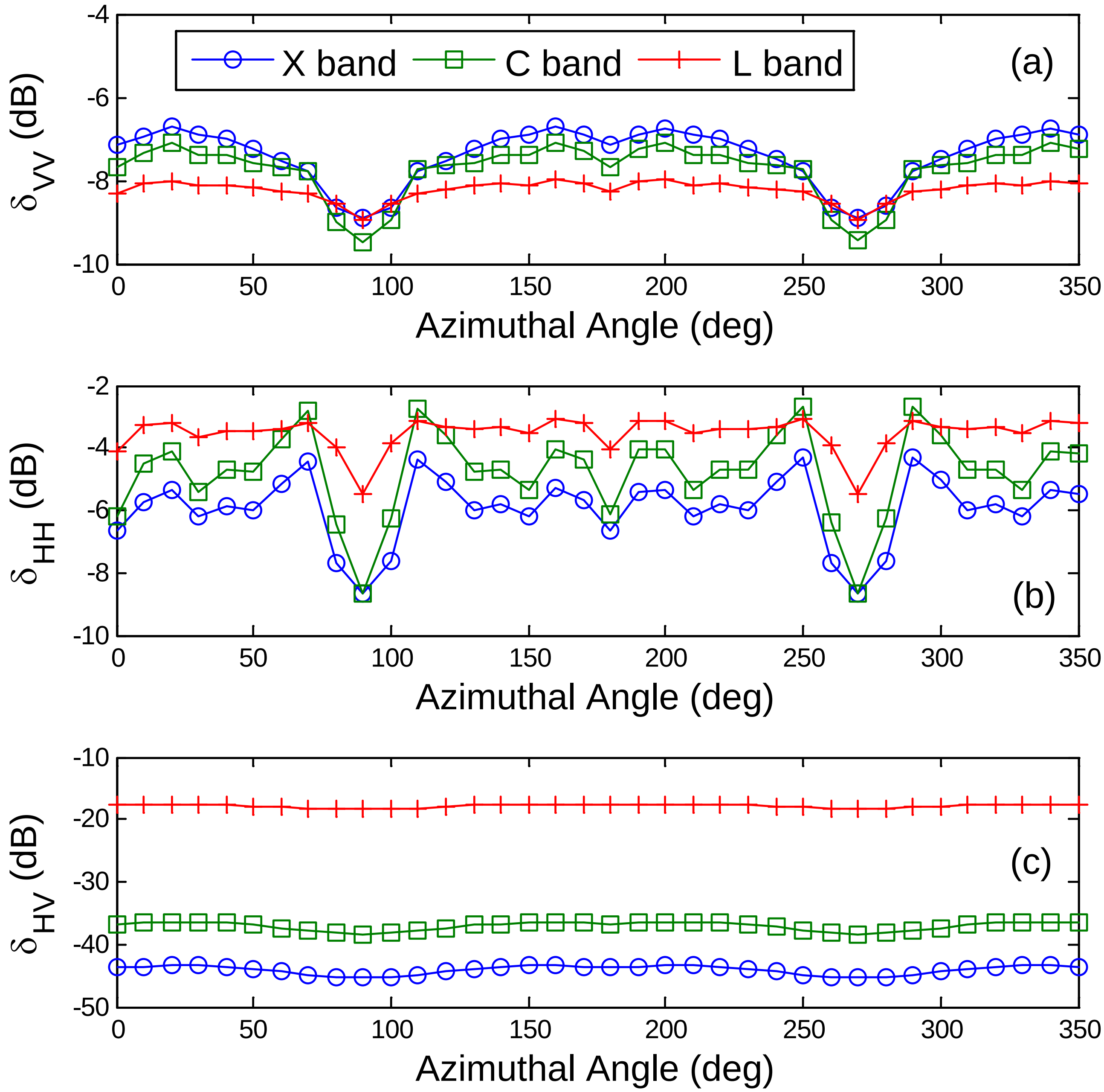

X band
C band
L band
(a)
(b)
(c)
δ_{VV} (dB)
δ_{HH} (dB)
δ_{HV} (dB)
Azimuthal Angle (deg)
Azimuthal Angle (deg)
Azimuthal Angle (deg)
-4
-6
-8
-10
-2
-4
-6
-8
-10
-10
-20
-30
-40
-50
0
50
100
150
200
250
300
350

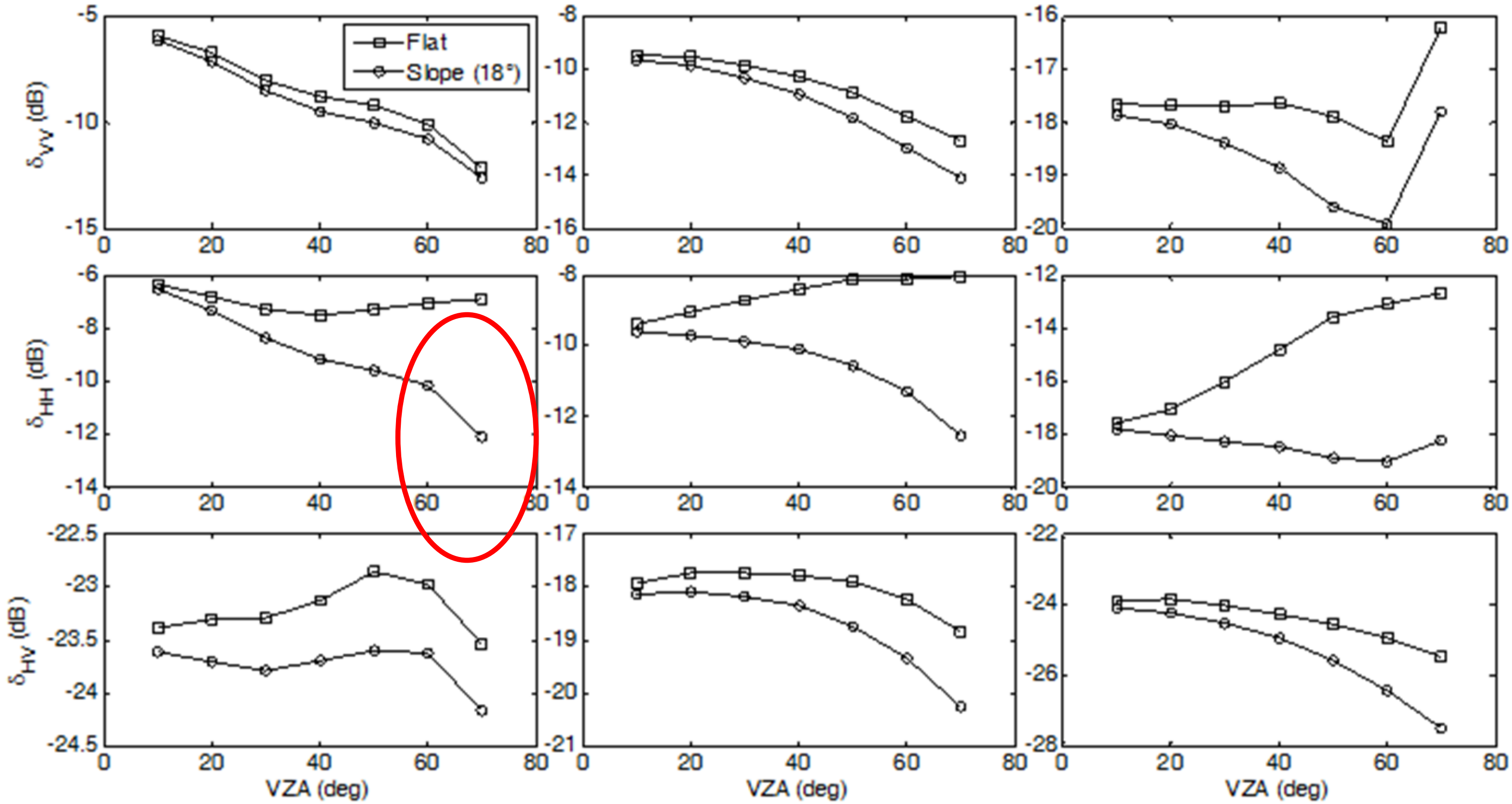

Figure 13.Slope effect on BSCs; band is from left to right, which is C, L and P- band respectively; polarization is from top to bottom, which is VV, HH, and HV respectively.

Slope reduced BCS

6. Summary

- A unified 3D model for optical and radar simulation is possible and beneficial
- Porous object is the common basic unit.
- Backscattering coefficients are sensitive to row structure and slope

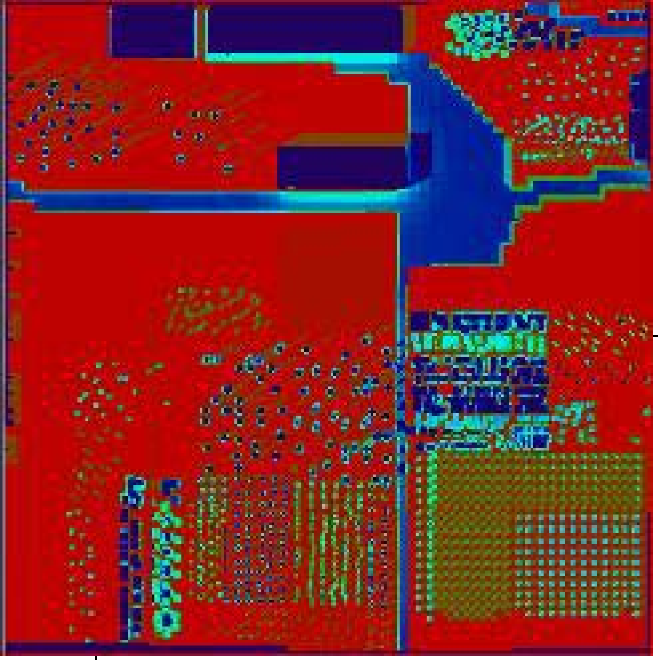

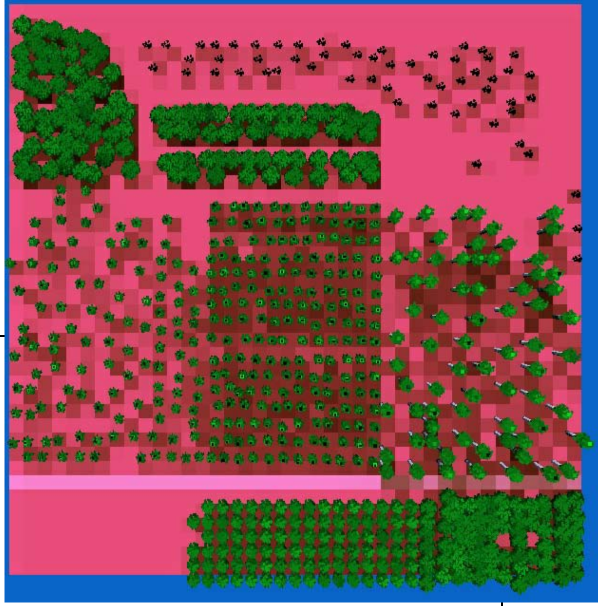

Thanks.

RAPID website

http://rapidmodel.wikispaces.com/

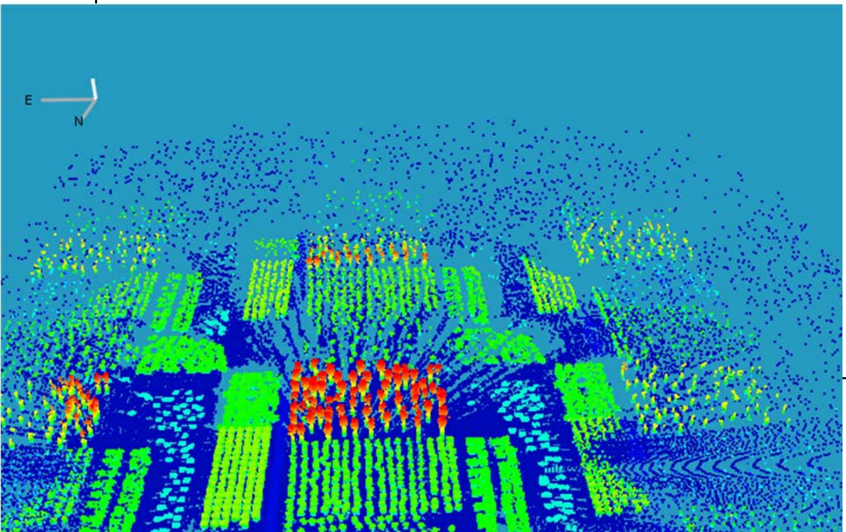

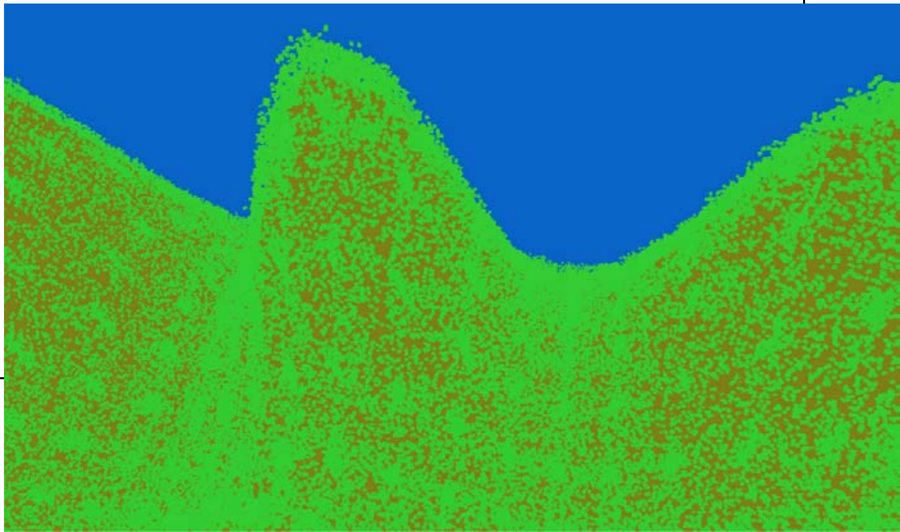

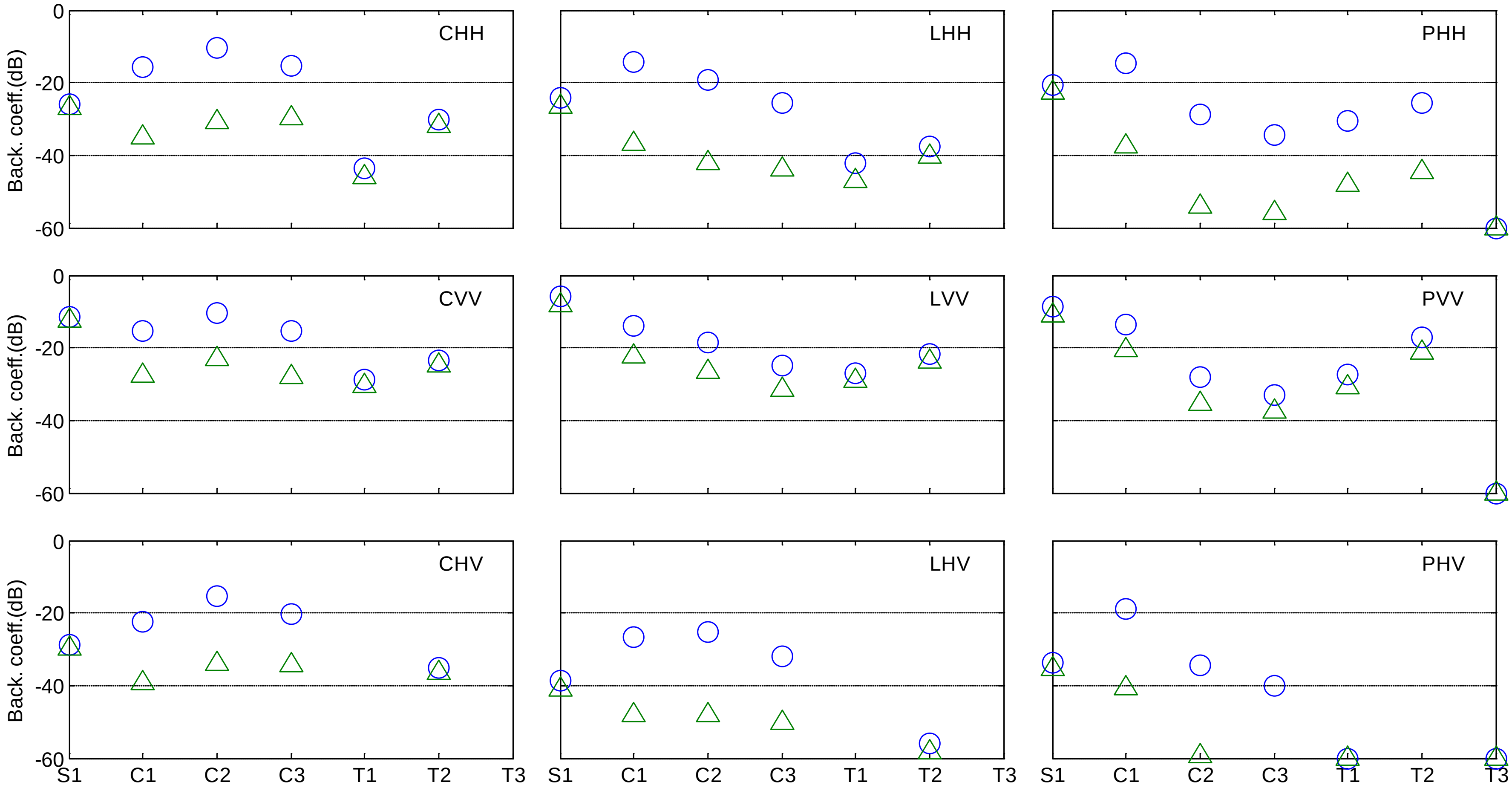

Figure 7. Contributions of canopy components (x axis) including crowns (C1= SLI, C2= Large CP, C3=Small CP), trunk (T1=SLI, T2= Large CP, T3=Small CP), and soil (S1) to the backscattering (y axis, circles for total, triangles representing multiple scattering) in three bands at HH, VV and HV polarizations.

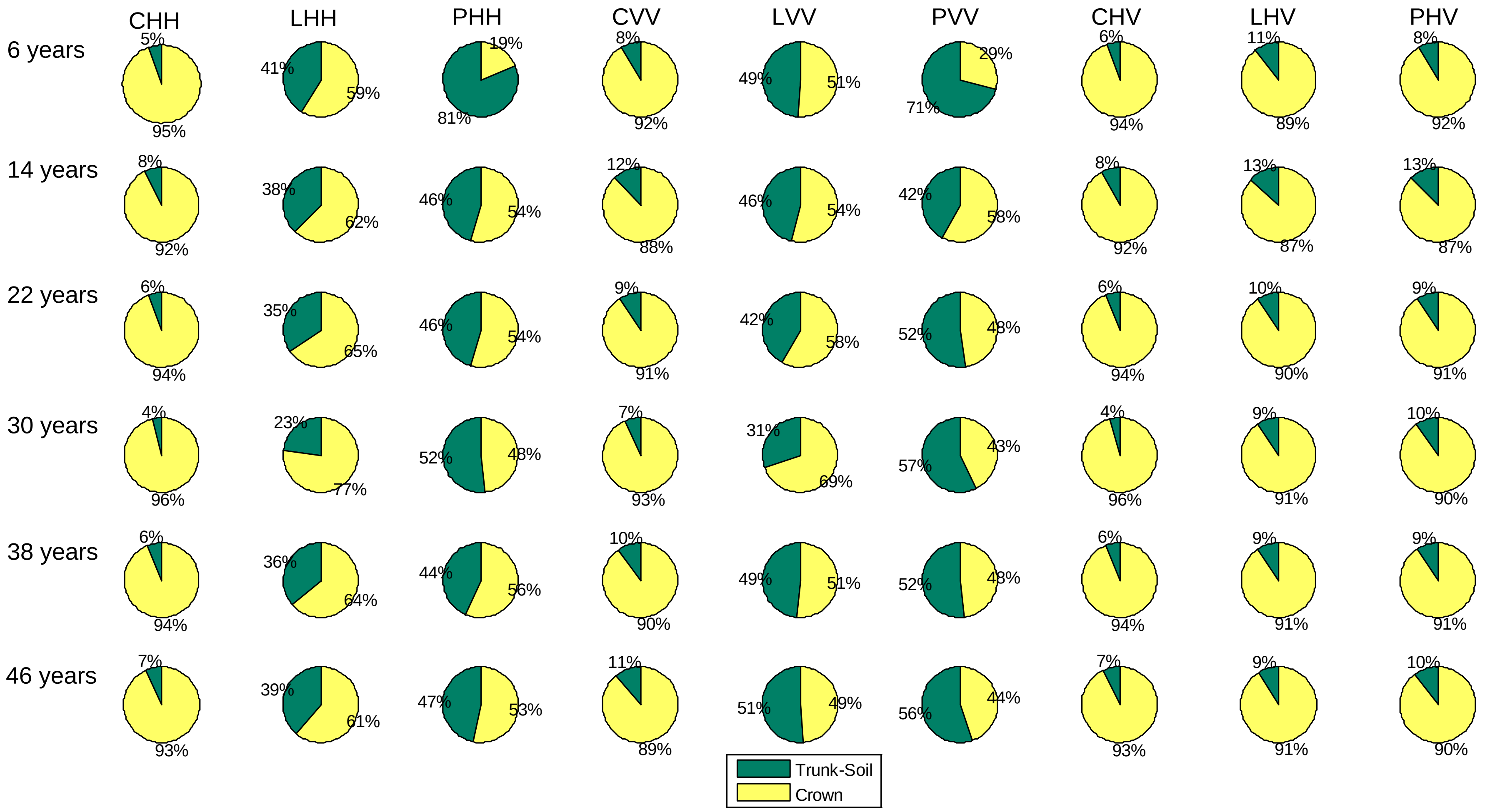

Figure 10. Contribution ratios between trunk-soil interactions (blue) and crown scattering (yellow) for six ages in three bands at HH, VV, and HV polarizations.